Tyndall
National Institute
Instituúid Náisiúnta

MEMS Energy Harvesting & Conversion Devices enabled by patterned Super-magnets leading to Internet of Things (IoT)

Prof. Saibal Roy

Research Professor – Physics Department
National University of Ireland- University College Cork (UCC)
A S Paintal Chair Professor of Engineering - INSA
Head: Micropower Devices and Nanomagnetics Group
Tyndall National Institute, Cork, Ireland
Email: Saibal.roy@Tyndall.ie

EnerHarv 2022
Raleigh, Durham, USA, 5-7 April 2022

UCC University College Cork, Ireland Coláiste na hOllscoile Corcaigh
Ireland's European Structural and Investment Funds Programmes 2014-2020 Co-funded by the Irish Government and the European Union
European Union European Regional Development Fund

Outline

- ❖ Powering IoT – Vibration (mechanical) Energy Harvesting (VEH)
- ❖ Electromagnetic (EM) Vibration Energy Harvesters
  – Linear (narrowband) to Nonlinear (wideband)
- ❖ Scaling Issues of EM-VEH Devices: MESO to MEMS scale
  – Challenges and Roadmaps
- ❖ Power conversion - Employing Micro-Nano-Magnetics
- ❖ Roadmap and Future Directions

Powering IoT - Vibration (mechanical) Energy Harvesting

Internet of Things (IoT) & Energy Harvesting

Tyndall National Institute
Institiúid Náisiúnta

Internet of Things (IoT) – Wireless sensors/nodes connecting things / devices to internet

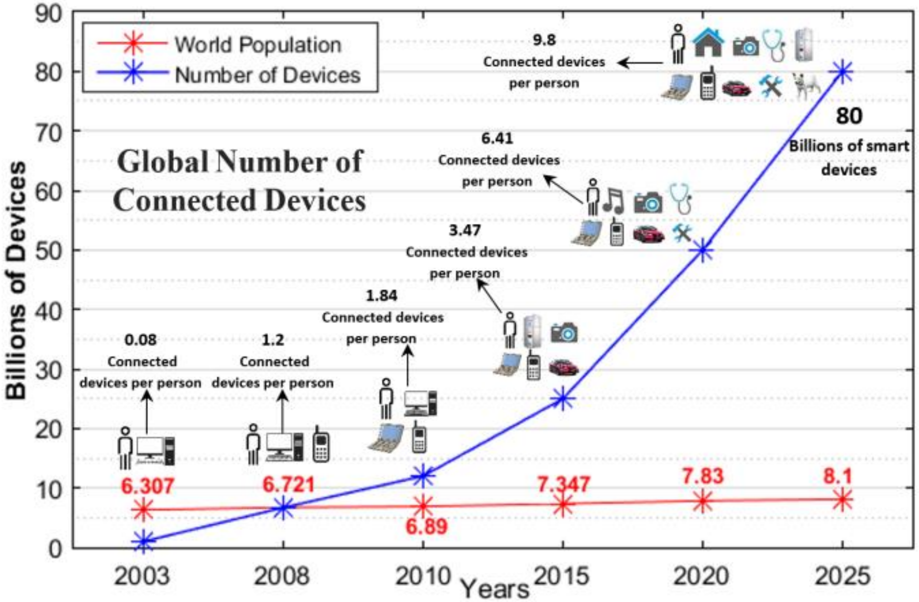

Farhan et al., Energy Efficiency for Green Internet of Things (IoT) Networks: A survey, Network 2021, 1, 279-314

Wireless Sensor Nodes & associated Networks

Building blocks of IoT

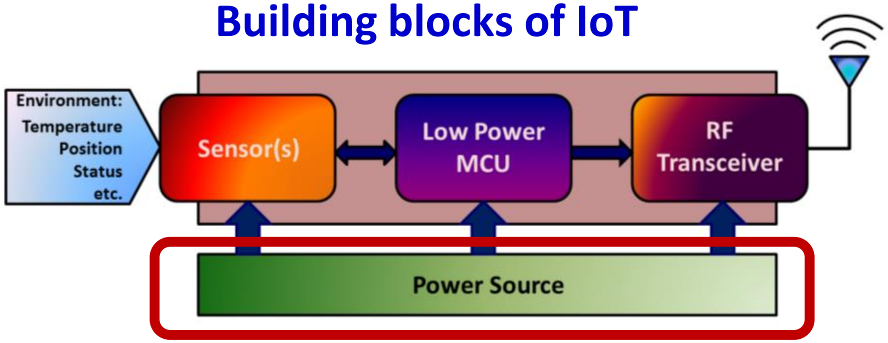

Self-powering?

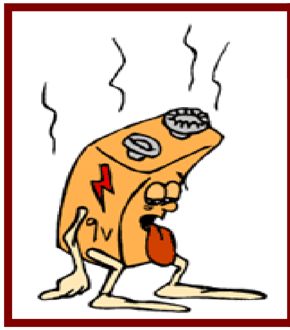

Batteries

Not suitable for 'fit-and-forget' Applications! Costs? Pollutions?

Energy Harvesting

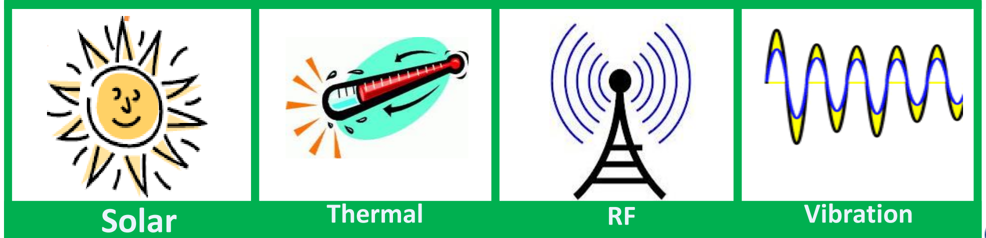

Vibration Energy Harvesting (VEH)

Mechanical energy is most easily accessible – Ambient Vibrations
Low amplitude vibrations can be found in every sphere of life – Huge Opportunity

Acoustic Emission Monitoring System

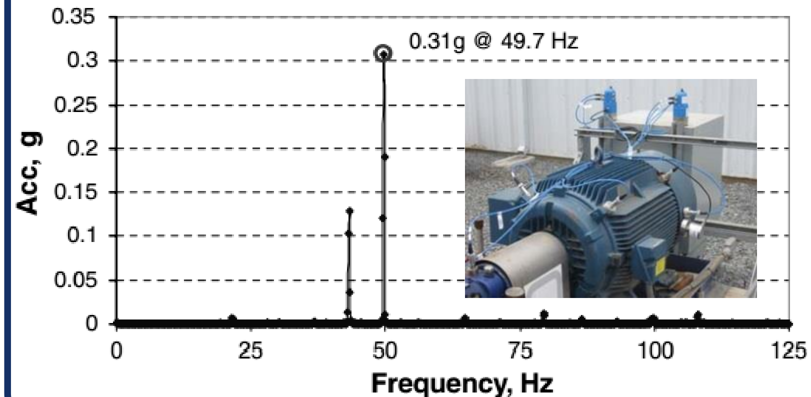

S. Beeby et al, J. Micromech. Microeng. 17, 1257–1265 (2007)

Railcar Application

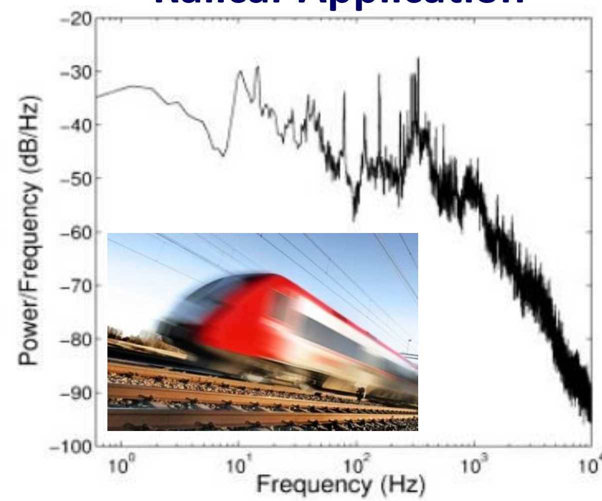

H. Vocca et al., Kinetic energy harvesting, in FAGAS G. (ed.), ICT Energy Concepts Towards Zero Power ICT, pp. 25-48 (2014)

Tyre Pressure Monitoring System

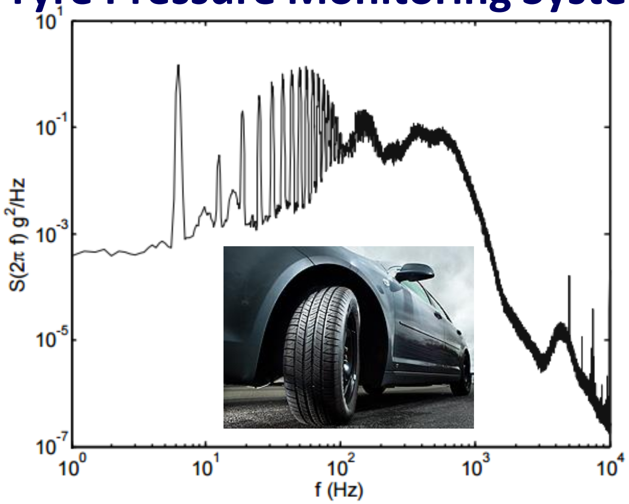

M. Löhndorf et al., Proc. PowerMEMS 2007, pp 331–4 (2007)

Cardiac Implant Devices

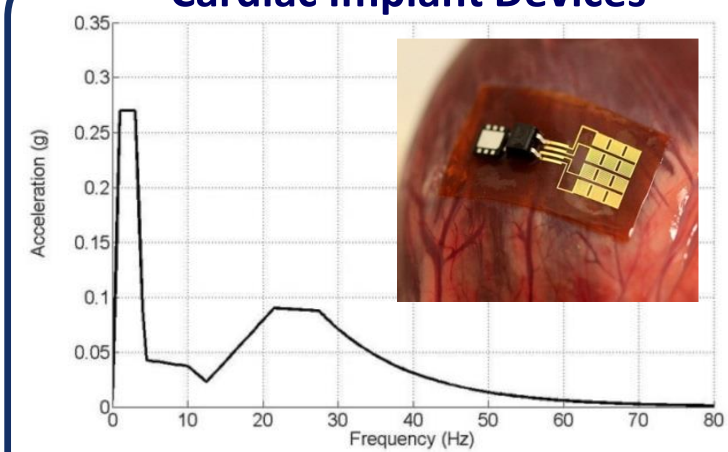

M. Deterre et al., Proc. Symp. DTIP MEMS/MOEMS, pp. 387–391 (2011)

Different Transduction Methods

Tyndall National Institute
Institiúid Náisiúnta

Comparison of Different Transduction Methods

Electrostatic	Piezoelectric	Electromagnetic
• Based on **changing capacitances** of the charged plates. • The voltage will change as the capacitance changes.	• **Charge displacement** occurs when the material is strained. • Thus a potential difference is obtained.	• Based on the **Faraday's Law of Induction.** • When a conductor moves through a magnetic field, a potential difference is induced.
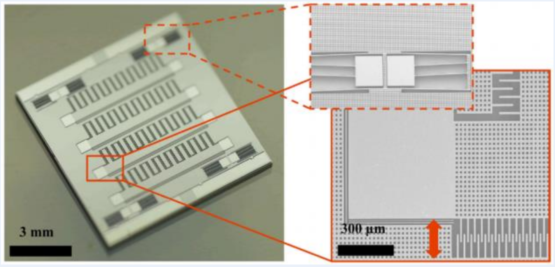	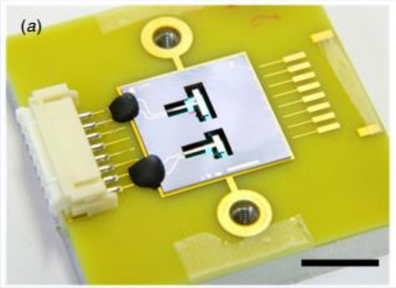	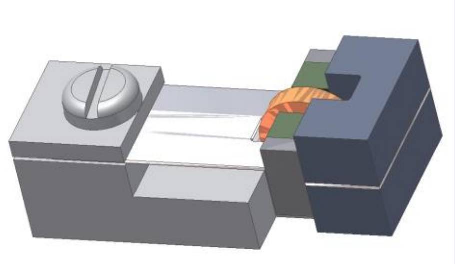
• Suitable for MEMS • Low o/p voltage at high operational voltage • High impedance values	• Active materials for fabrication, brittle. • High Voltage, Low Current • High Impedance values	• Do not need any extra component. • High Current, Low Voltage • Challenging in MEMS

Inertial Energy Harvesting System

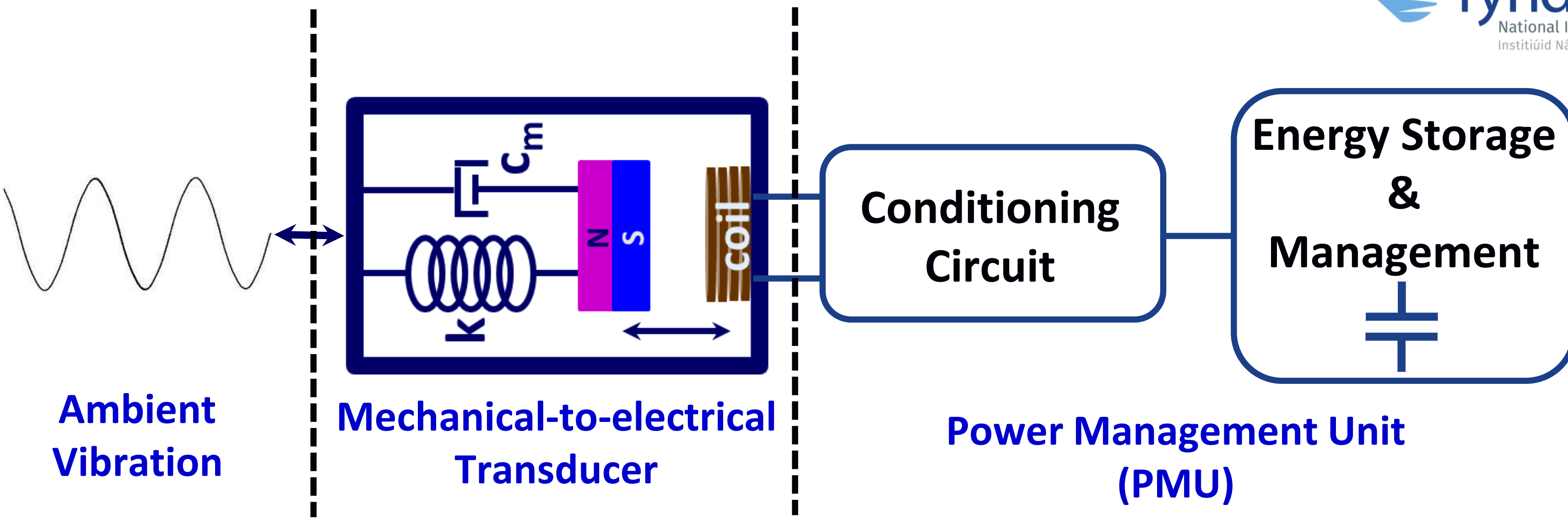

Second Order Spring Mass Damper System

$$m\ddot{x}(t) + (c_m + c_e)\dot{x}(t) + kx(t) = -m\ddot{y}(t)$$

Power dissipated in the electrical damper

$$P_{elec} = \frac{c_e\left(\frac{\omega}{\omega_n}\right)^3 {Y_0}^2 \omega^3}{2\omega_n\left[\left\{2\rho_T\left(\frac{\omega}{\omega_n}\right)\right\}^2 + \left\{1 - \left(\frac{\omega}{\omega_n}\right)^2\right\}^2\right]}$$

At Resonance:

$$P_{elec}\big|_{\omega=\omega_n} = \frac{c_e m^2 {Y_0}^2 {\omega_n}^4}{2(c_m + c_e)^2}$$

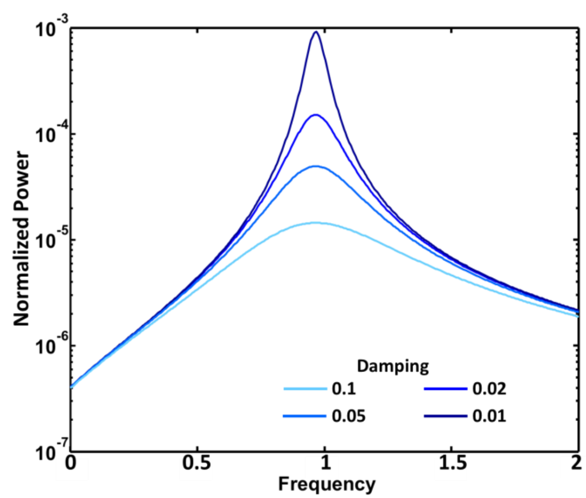

Inertial Energy Harvesting System

Tyndall National Institute
Institiúid Náisiúnta

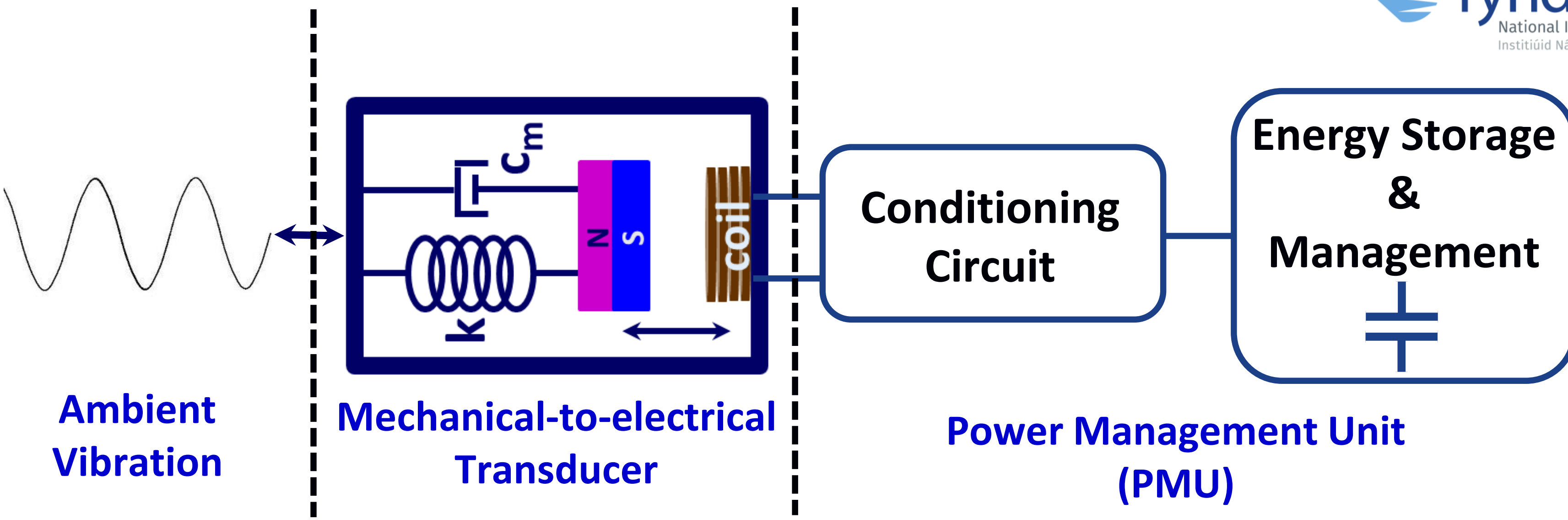

Principle governing EM generators is Faraday's Law

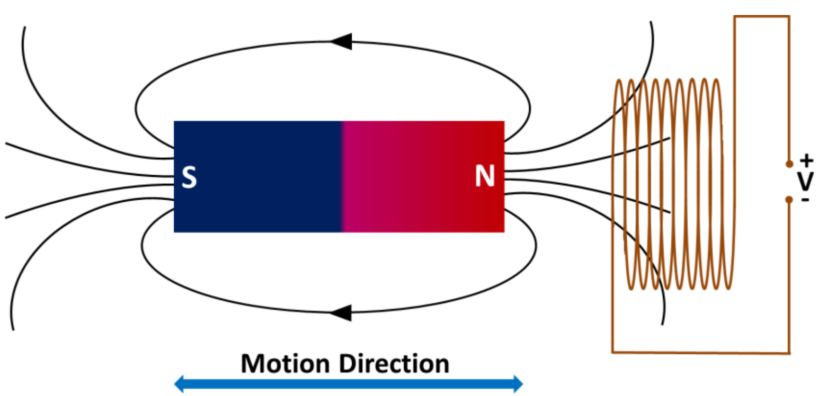

$$\text{EMF (V)} = -N\frac{d\Phi}{dt}$$

Induced voltage $V_o = Z_{max}\omega_n N \frac{d\Phi}{dz}$

Load Voltage $V_L = V_o \frac{R_L}{(R_L + R_C)}$

Power delivered to load $P_L = \frac{{V_L}^2}{2R_L}$

Electromagnetic (EM) VEH:
Linear (narrowband) to Nonlinear (wideband)

Commercially Available EM VEHs

Tyndall National Institute
Institiúid Náisiúnta

EnOcean Light Switch

- Energy output 120-210 µJ at 2V
- Dimension: 29 X 19 X 7 mm^3
- Application: Wireless Light Switch

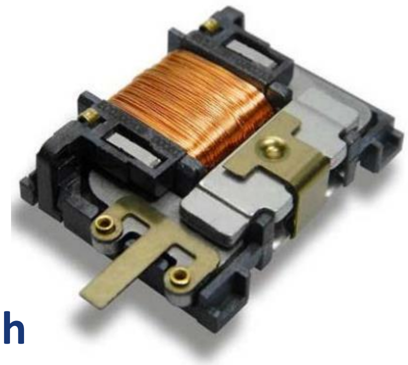

Perpetuum Energy Harvester

- Bulky – weigh 1.03 kg
- 4.2 mW, 8V, 0.525 mA @0.05g
- Applications: Railroad, Industrial monitoring

ReVibe Energy Harvester

- modelD: 61 mm (height) x 32 mm (diameter)
- 2 mW @ 60 Hz and 0.1g
- Application: Industrial monitoring

Remarks:

- Majority of them are bulky, heavy systems
- Most commercial products are linear or single frequency
- Focuses on structural, infrastructure and industrial monitoring applications
- Need for miniaturization is clear

Macro/Mesoscale EM VEHs – SOA in literature

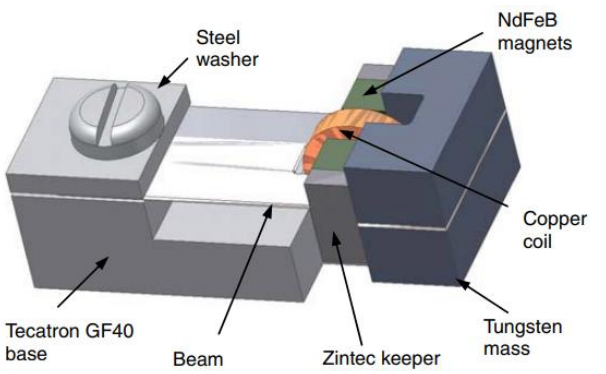

S. P. Beeby et al., J. Micromech. Microeng., 17, 1257 (2007)

- Volume – 0.15 cm^3
- Power – 0.046 mW @ 0.06g
- Frequency – 52 Hz

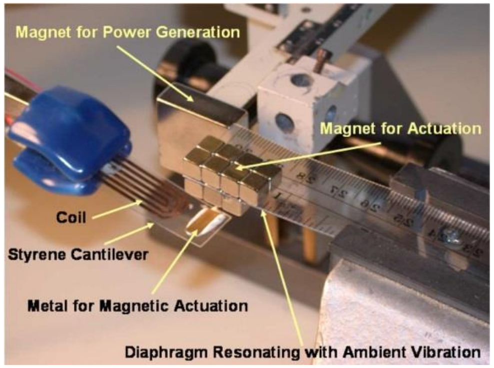

H. Kulah, H. Najafi., IEEE Sens., 8(3), 261 (2008)

- Volume – 0.3 cm^3
- Power – 120 μW @ 1g
- Frequency – 64 Hz

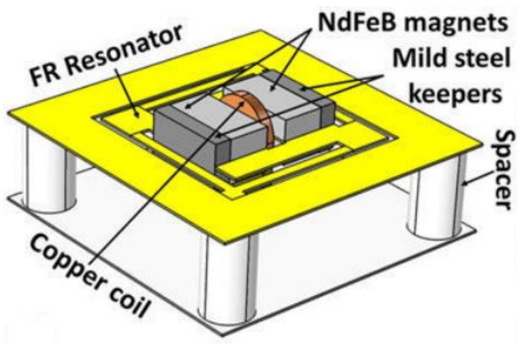

D. Mallick, S. Roy, Sens. Act. A, 226, 154 (2015)

- Volume – 2.65 cm^3
- Power – 0.5 mW @ 0.3g
- Frequency – 58.6 Hz

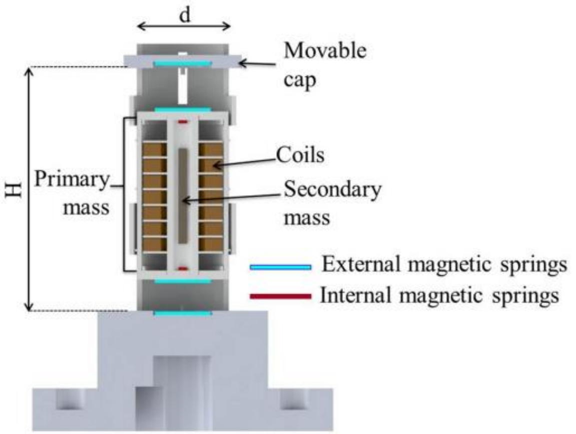

V. Nico et al., Appl. Phys. Lett., 108, 013902 (2016)

- Volume – 12.1 cm^3
- Power – 2.75 mW @ 0.4g
- Frequency – 11.25 Hz

- **Volume – 0.1 cm^3 to higher**
- **Discrete components assembled together – Fine machining**
- **Magnet array to increase flux density**
- **Lower Frequencies – Application relevant**
- **Reasonable Power Density**

Magnetic Flux Distribution

Suitable Magnet Coil Arrangement – High Power Generation

Halbach Array

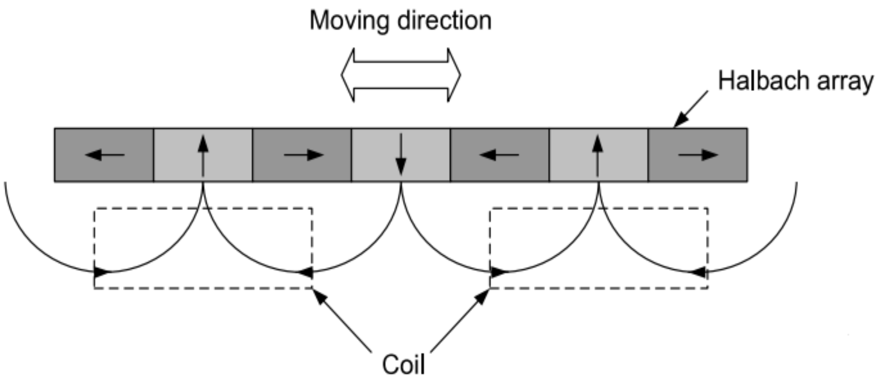

D. Zhu et al., Smart Mater. Struc., 21(7), 075020 (2012)

Alternate Oppositely Polarized Magnets

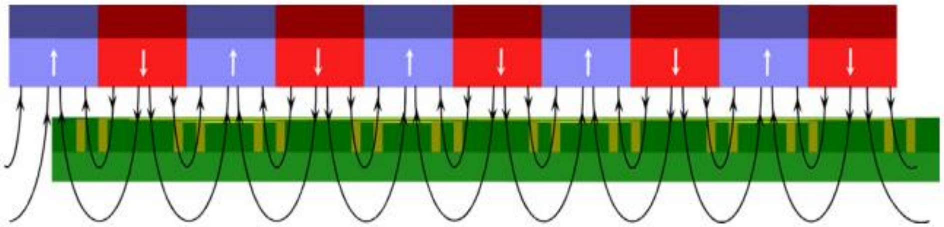

S. Roundy, E. Takahashi, Sens. Act. A:Phys., 195, 98 (2013)

Closed Magnetic Circuit

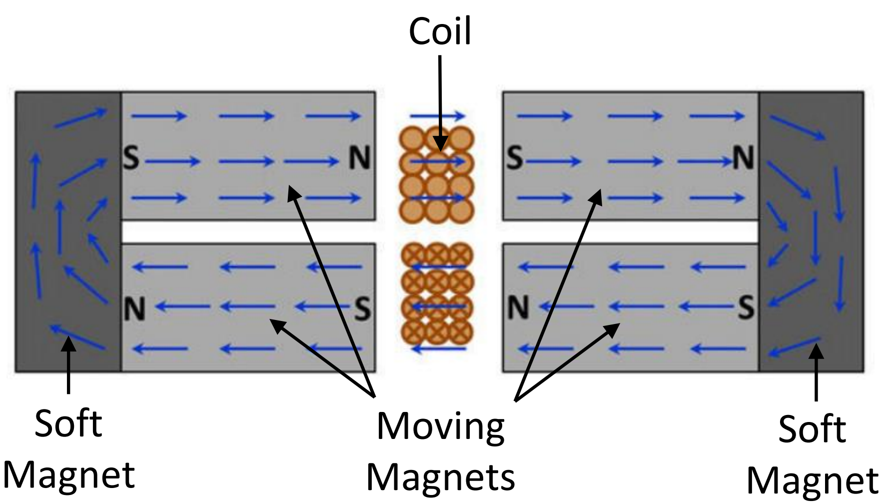

D. Mallick, S. Roy et al., Smart Mater. Struc., 24(12), 122001 (2015)

Double Cell Configuration

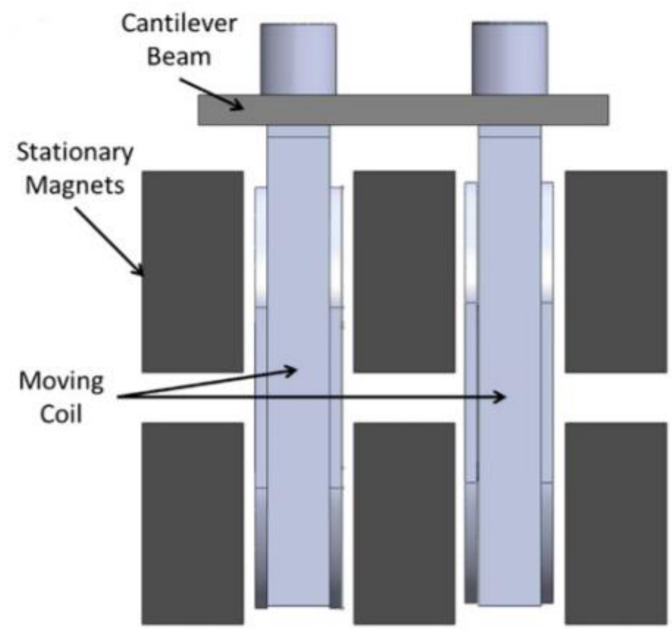

A. Marin et al., J. Phys. D: Appl. Phys. 44, 295501 (2011)

Vibration Sources – low frequency

Resonant, Impulse, Shock

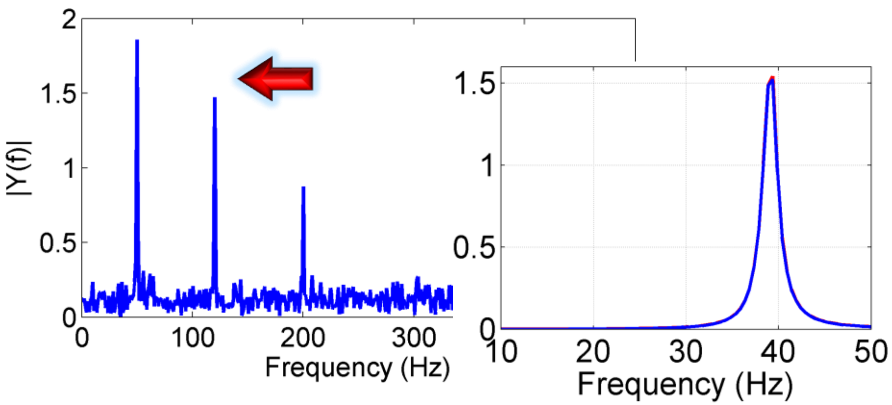

Linear VEH

Broadband, Random, Noise

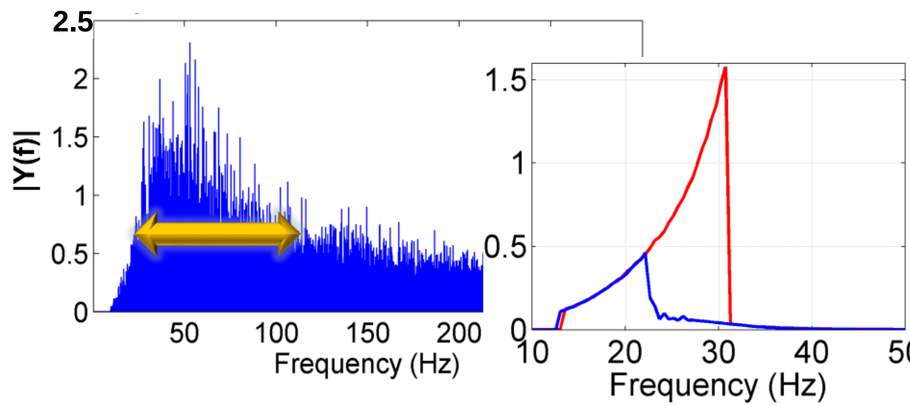

Wideband VEH

Nonlinear Energy Harvesting

Nonlinearity introduced through modified stiffness of the devices → **broader frequency response**

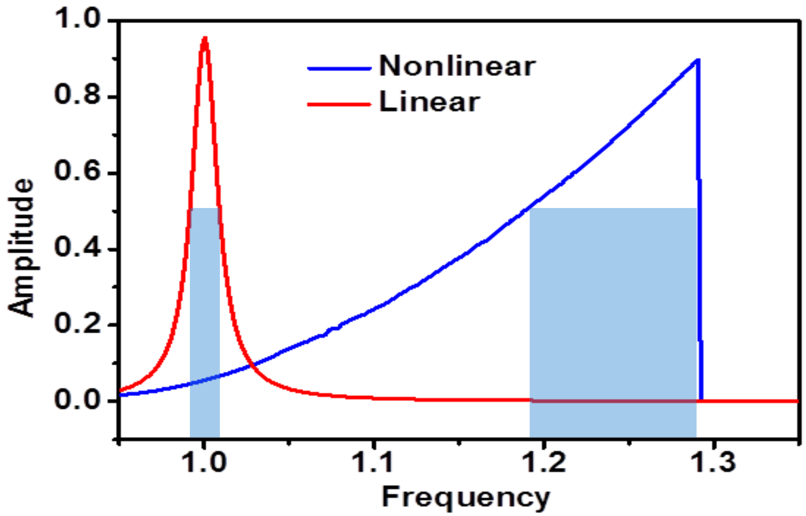

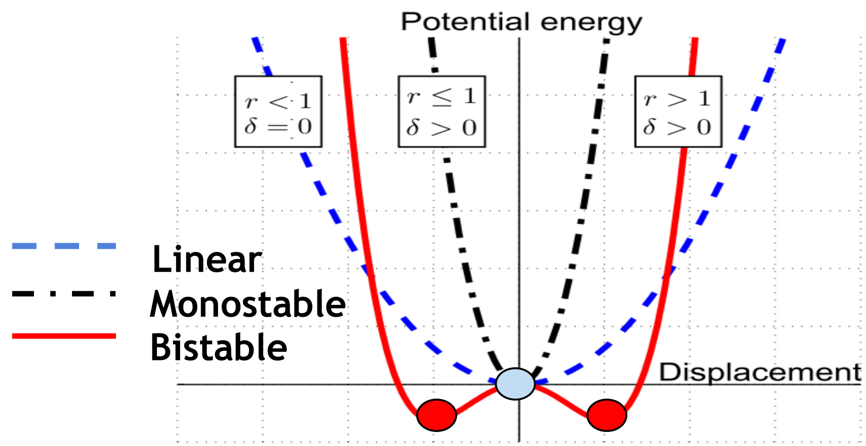

$$\ddot{x} = -\frac{dU(x)}{dx} - \gamma\dot{x} + f(t)$$

$$F(x) = -kx - k_n x^3$$

$$U(x) = -\frac{1}{2}\alpha(1-r)x^2 + \frac{1}{4}\beta x^4 \qquad \delta = \frac{\beta}{\alpha}$$

α, β are constants

r - determines nature of nonlinearity

Miniaturized Nonlinear EMPG Systems

Mono-stable Nonlinear EMPG

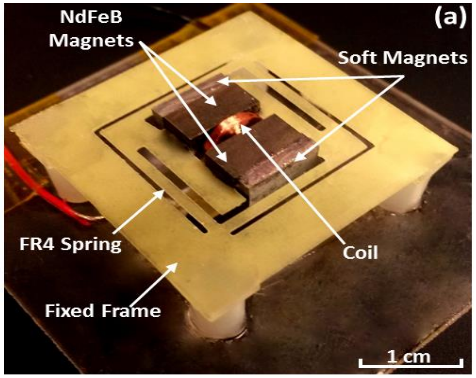

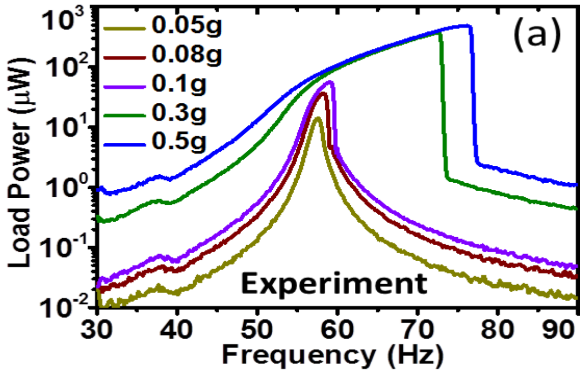

- Mono-stable nonlinearity from stretching strain in addition to bending of fixed-guided beams.
- 0.5 mW of peak power under 0.5g acceleration

Bi-stable Nonlinear EMPG

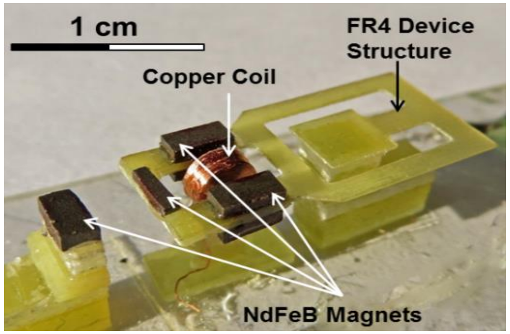

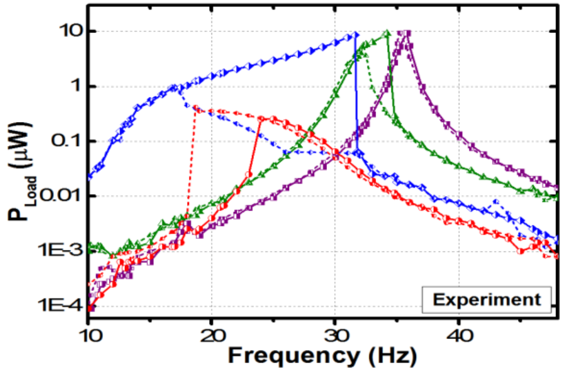

- Bi-stable nonlinearity from magnetic repulsive interaction.
- 29μW of power under 0.5g acceleration.

❖ D Mallick, A Amann, S Roy; Smart Materials and Structures 24, 015013, (2014)
❖ S Roy, P Podder, D Mallick; IEEE Magnetics Letters 7, 1-4, (2015)

Combined bistable-quartic nonlinearity- Meso scale

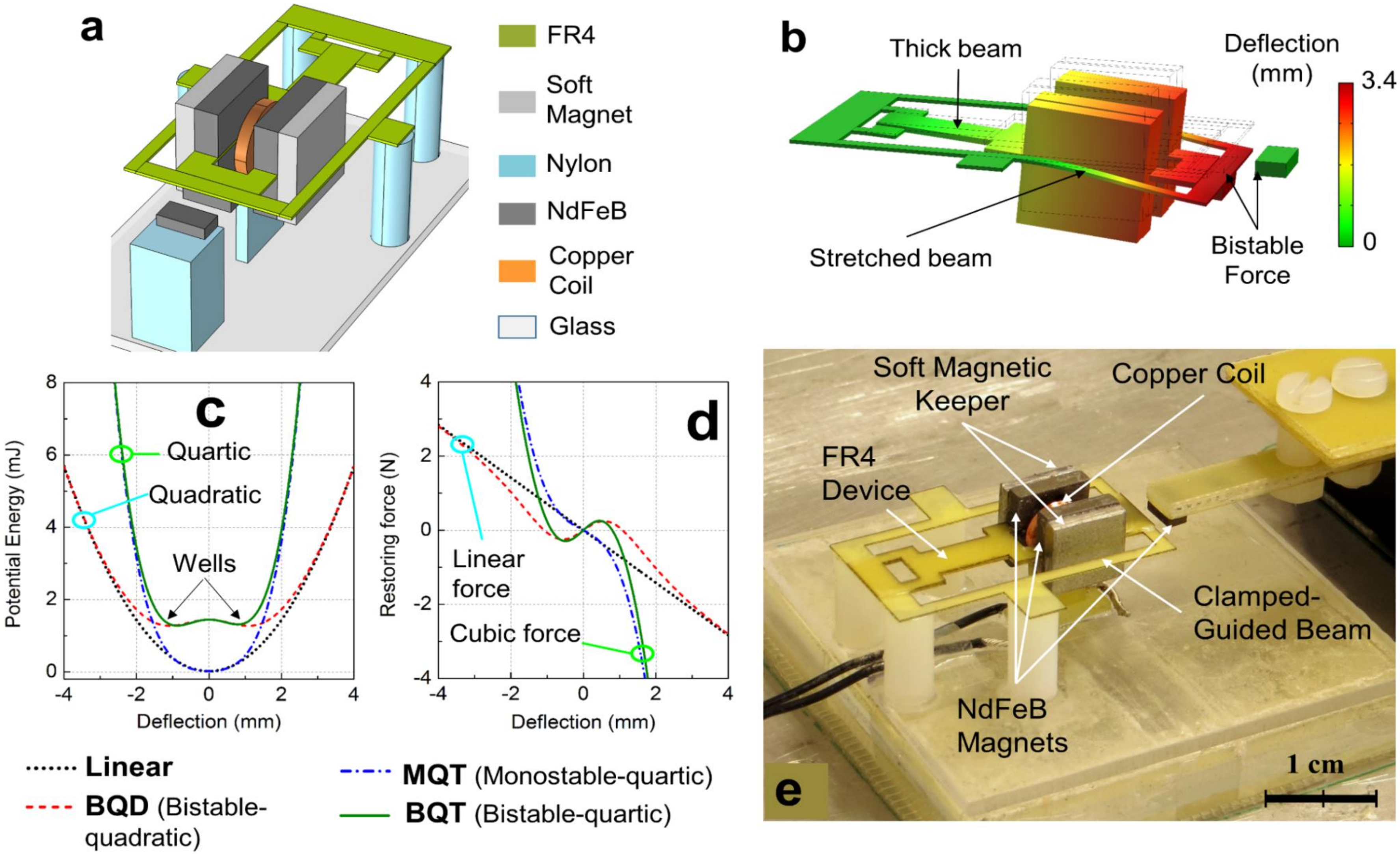

- Stretching of the clamped-guided pair of beams contributes to mono-stable cubic nonlinearity
- Bi-stable nonlinearity is incorporated by the repulsive magnetic force at the tip of the cantilever
- 1403 μW of power at 1g

❖ P Podder, D Mallick, A Amann, S Roy; Scientific Reports; 6, 37292, (2016)

❖ S Roy, P Podder, D Mallick, A Amman; Patent granted – EP 3311472, Jan 2020; US 10971986B2, April 2021

Electromagnetic (EM) VEH:
Meso to MEMS Scale

MEMS-scale EM VEHs – SOA in literature

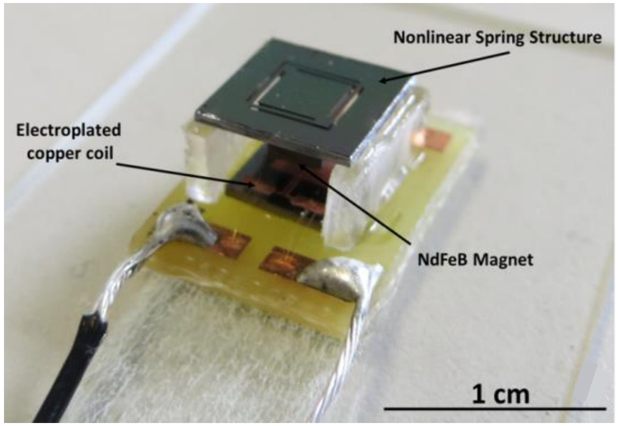

D. Mallick et al., J. Microelectromech. Syst., 26(1), 273 (2016)

- Volume – 0.1 cm^3
- Power – 2.8 µW @ 0.5g
- Frequency – 630 Hz

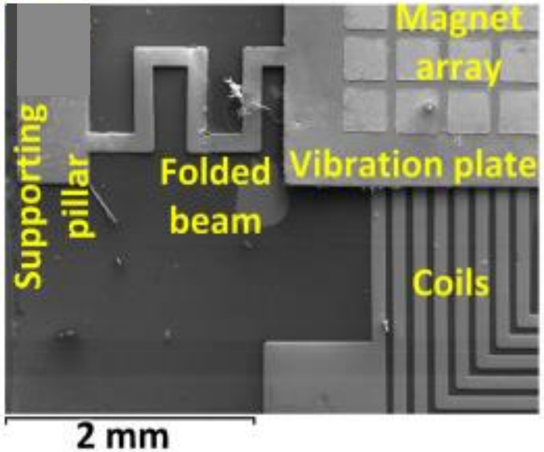

M. Han et al., Sens. Act. A: Phys., 219, 38 (2014)

- Volume – 67.5 mm^3
- Power – 10 nW @ 1g
- Frequency – 48 Hz

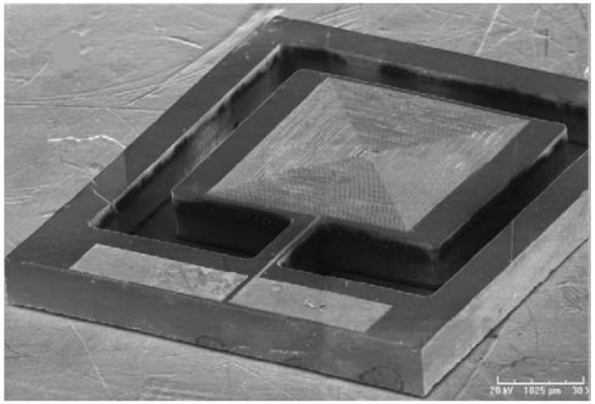

S. Kulkarni et al., Sens. Act. A: Phys., 145, 336 (2008)

- Volume – 0.1 cm^3
- Power – 23 nW @ 1g
- Frequency – 9830 Hz

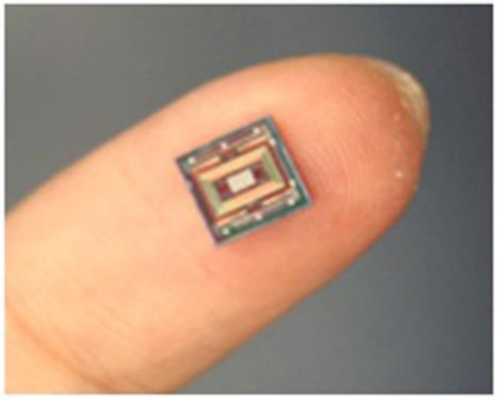

H. Liu et al., Appl. Phys. Lett., 104, 053901 (2014)

- Volume – 0.16 cm^3
- Power – 0.06 nW @ 1g
- Frequency – 384 Hz

❖ **MEMS – micro-scale features**

❖ **Semi (most) or Fully (few) batch-fabricated**

❖ **Si or non-Si (PDMS, electroplated Ni) suspension systems**

❖ **Bulk Magnets**

Benchmarking the MEMS EM VEHs

Normalized Power Density(NPD)

$$= \frac{\text{Power}}{\text{Acceleration}^2.\text{Volume}}$$

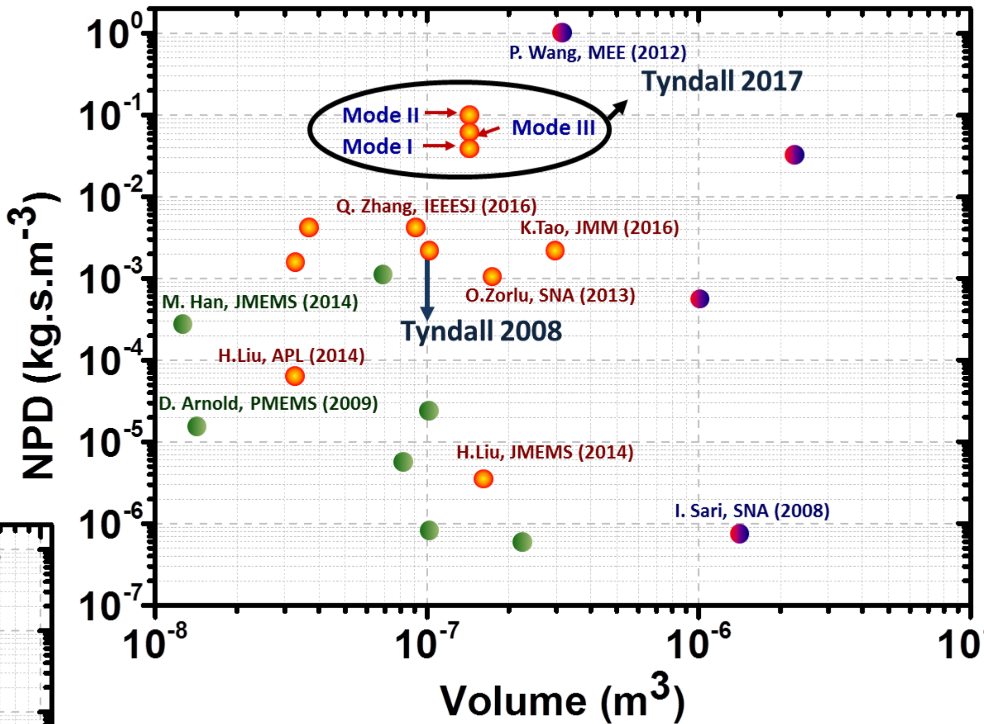

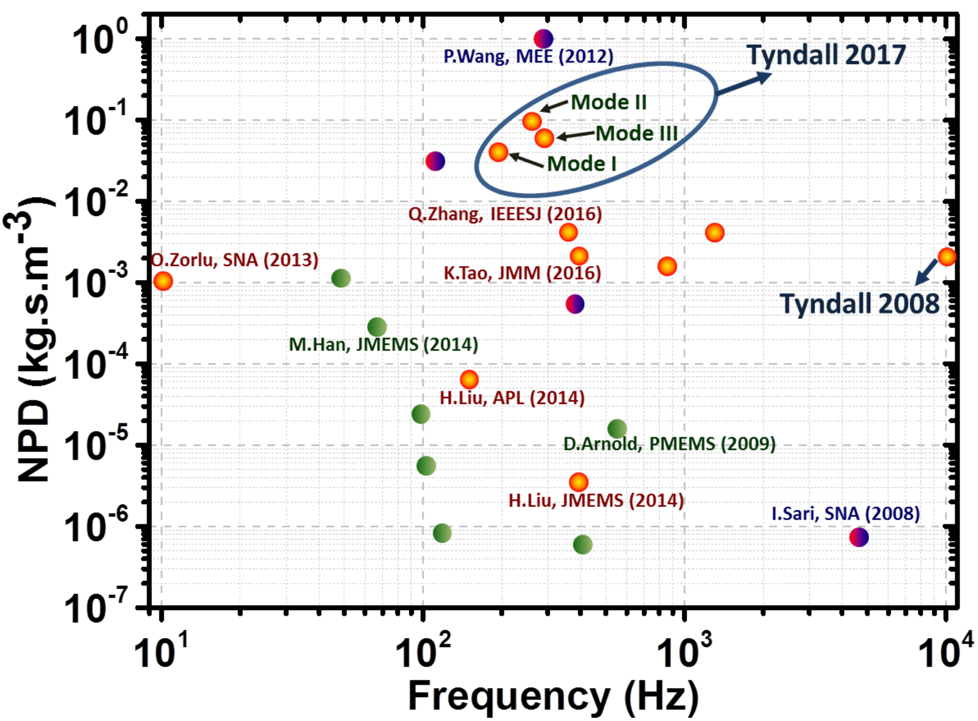

- MEMS Suspension only
- MEMS Suspension with micro-coil
- Fully MEMS integrated

D. Mallick, S Roy, Sens. Act. A: Phys., 264, 247 (2017)

Scaling remains the main issue

Tyndall National Institute
Institiúid Náisiúnta

MEMS reduces cost

Trade Off: Size vs Effectiveness

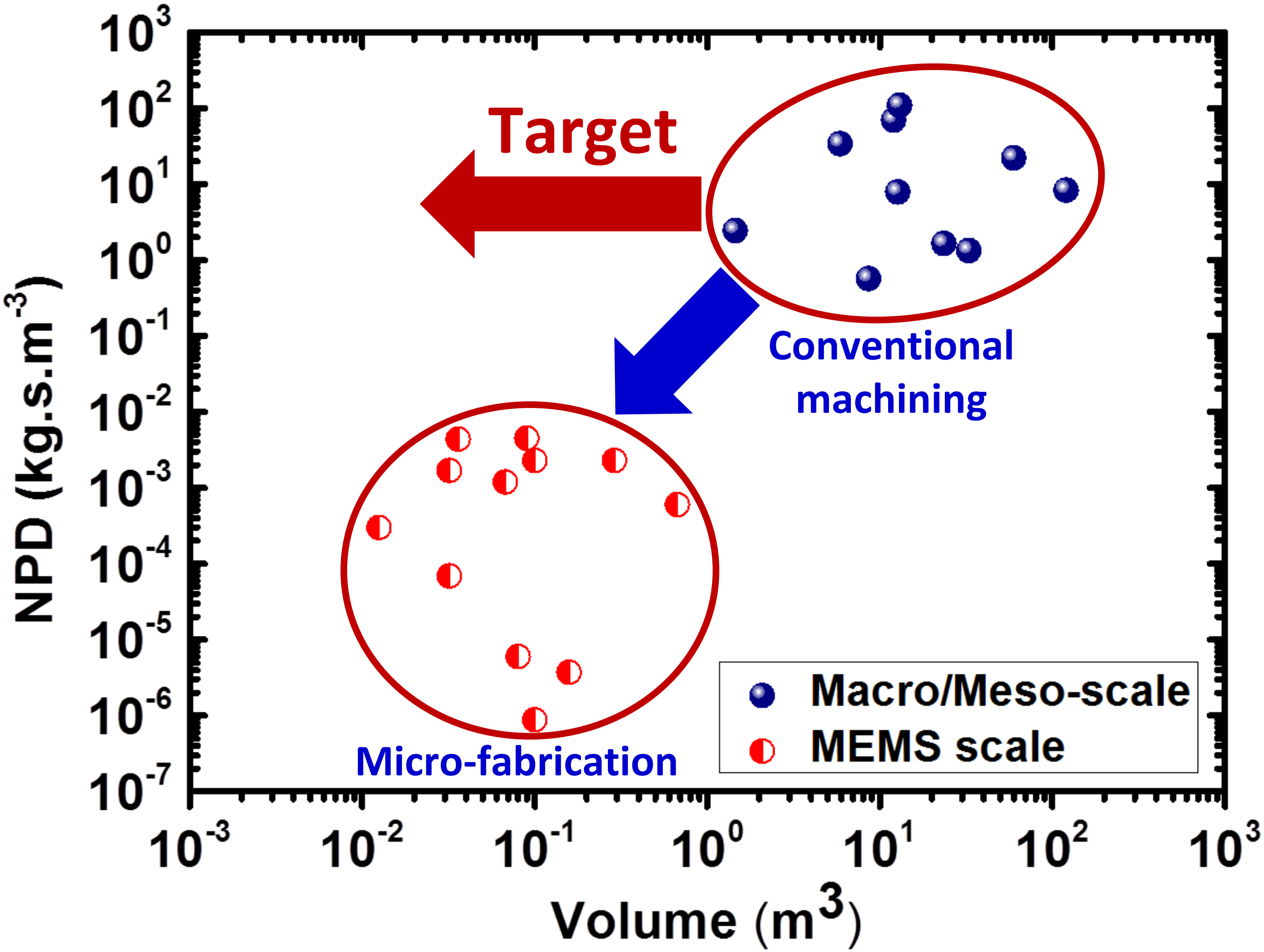

Scaling Issues of EM VEH Devices: Challenges and Roadmaps

Scaling of EM VEHs

Maximum load power generated by a EM Generator at resonance for matched load

$$P_L = \frac{m^2 {a_0}^2}{8c_m(\frac{R_C c_m}{\gamma^2} + 1)}$$

Where, $\gamma = N\frac{d\varphi}{dx}$ is the electromagnetic coupling

$m \propto L^3$
$c_m \propto L$
$\gamma \propto L$
$R_C \propto L^{-1}$
$\gamma^2 / R_C \propto L^3$

$$P_L \propto \frac{L^7 {a_0}^2}{L^2 + 1}$$

Case I: $c_m \ll \frac{\gamma^2}{R_C}$ For $R_C \rightarrow 0$

Coil damping dominates at large scale

$$P_L \approx \frac{m^2 {a_0}^2}{8c_m} \propto L^5 {a_0}^2$$

Case II: $c_m \gg \frac{\gamma^2}{R_C}$

mechanical damping dominates at small scale

$$P_L \approx \frac{\gamma^2 m^2 {a_0}^2}{8{c_m}^2 R_C} \propto L^7 {a_0}^2$$

Two asymptotic scaling laws can be obtained:

$P_L \propto L^5 {a_0}^2$ **For $L \rightarrow \infty$**

$P_L \propto L^7 {a_0}^2$ **For $L \rightarrow 0$**

D. P. Arnold, IEEE Trans Magn., 43(11), 3940 (2007)

Scaling of EM VEHs (II)

Let us take a look at the electromagnetic damping term

$$c_e = \frac{N^2 (\frac{d\varphi}{dx})^2}{R_C + R_L}$$

Number of Coil Turns

- Decreases with scaling
- Limited by technology

Magnetic Flux Linkage Gradient

- More important than flux density
- Magnetic flux density from PM scales independently of size
- Flux linkage gradient depends on area of the coil

If generator scales by factor b

- Flux density gradient increases by b
- Area of the coil decrease by factor b^2
- Flux linkage gradient decrease by b

Coil Resistance

Micro-fabricated Coil Resistance:

$$R_C = \frac{8\rho_{Cu}(d_0 + d_i)}{(d_0 - d_i)^2}(4N^3 - 4N^2 + N)$$

Rc is inversely proportional to the scaling factor

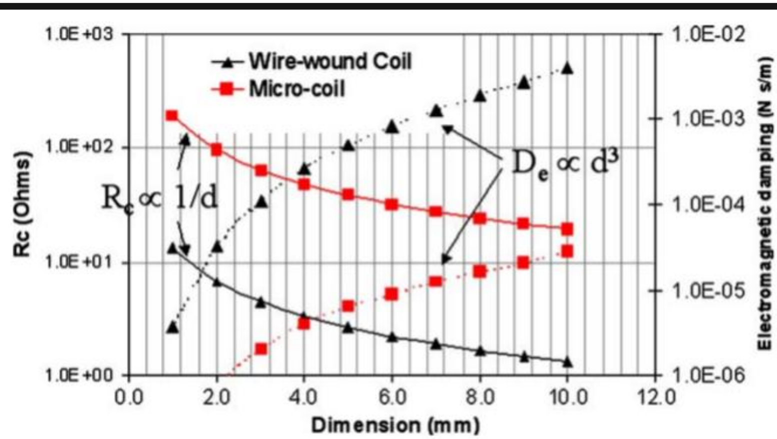

C. Saha et al., Microsyst Technol (2007) 13:1637–1645

Micro-fabricated Coils in EM-VEH

Single/Multi-layer micro-coils

Tyndall National Institute
Institiúid Náisiúnta

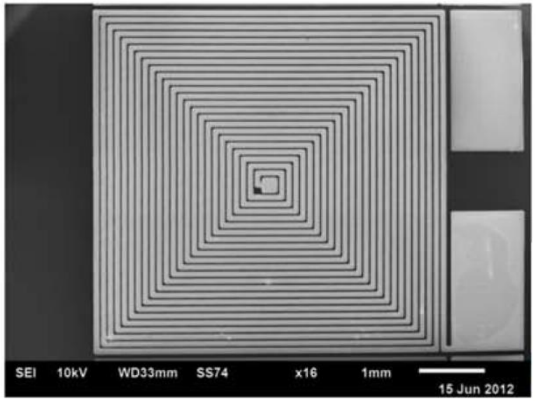

Electroplated Single Layer Copper Coil[1]

- 20 Turns,
- 3.6 Ω,
- 22 µm thickness

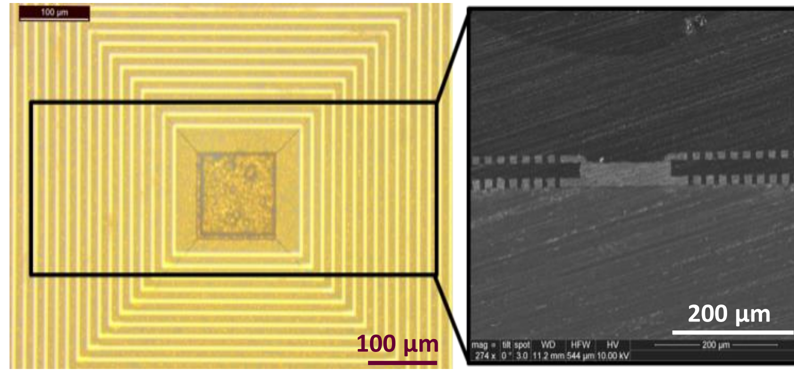

Electroplated Double Layer Copper Coil[2]

- 144 Turns,
- 190 Ω,
- 10 µm track width, spacing, thickness

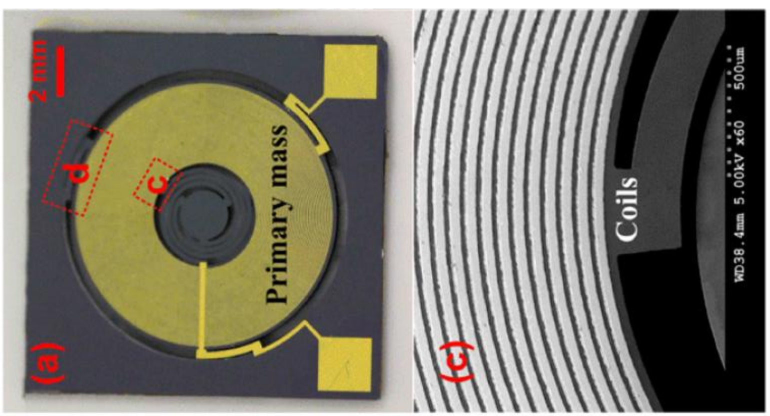

Sputtered Double Layer Cr/Au Coil[3]

- 57 Turns,
- 12.7 kΩ,
- 30/30width/spacing, 350 nm thickness

❖ Sputtered Al, Cr/Au coils – very thin, high resistance

❖ Electrodeposited Cu coils – thick, low resistance, low cost

1. Q. Zhang, E. S. Kim, Proc. IEEE, 102(11), 1747 (2014)
2. D. Mallick et al., J. Microelectromech. Syst., 26(1), 273 (2016)
3. K. Tao et al., J. Micromech. Microeng., 26, 035020 (2016)

Roadmap for Micro-fabricated Coils

Tyndall National Institute Institiúid Náisiúnta

Improving the packing density:

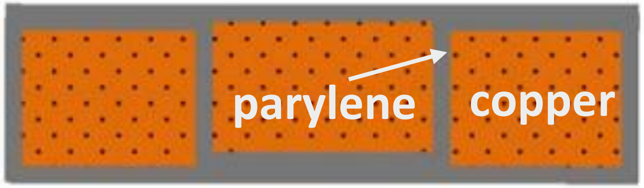

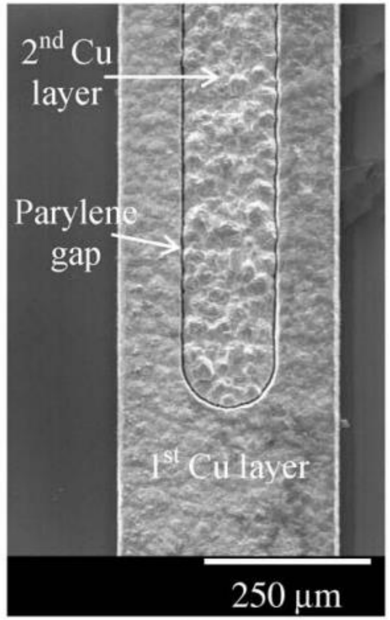

- Parylene conformally coated high density coil[1]
- Doubles the number of turns
- Complex fabrication process
- **Concern:** dielectric breaking - electrical short circuit

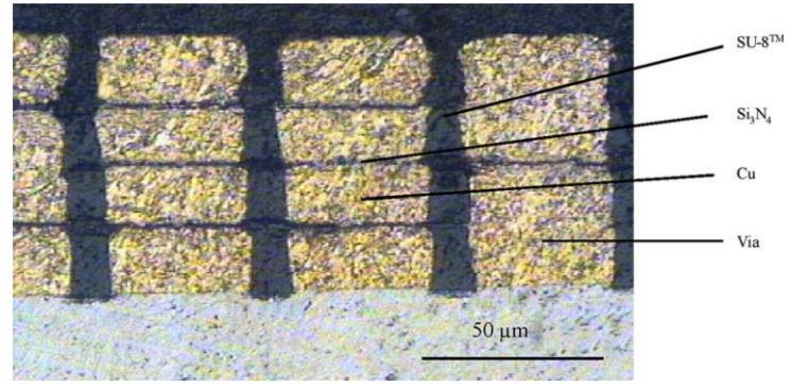

- Increasing the stack height[2]
- Increasing the aspect ratio (AR=w/h)
- Using standard lithography, it is possible to develop as high AR as 1:17 and 5 µm resolution[3]

MEMS compatible 3D coil[4]:

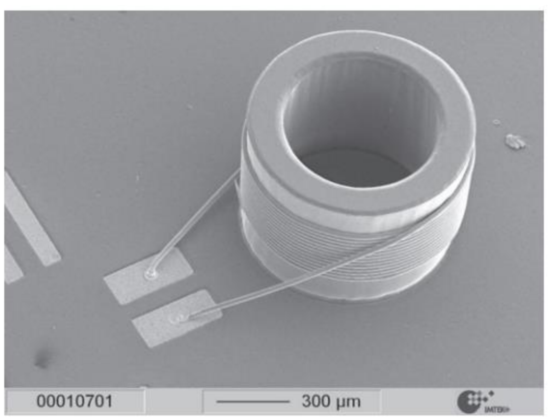

- Wire-bonded
- 3D solenoid structure
- Number of windings is limited by the post height

1. F. Herrault et al., J. Micoelectromech. Syst., 19(6), 1277 (2010)
2. C. Ruffert, H. H. Gatzen, Microsyst. Technol., 14, 1589 (2008)
3. R. Anthony et al., J. Micromech. Microeng. 26, 105012 (2016)
4. K. Kratt et al., J. Micromech. Microeng., 20, 015021 (2010)

Integrated Permanent Magnets

Key Challenge: Permanent Magnet Integration

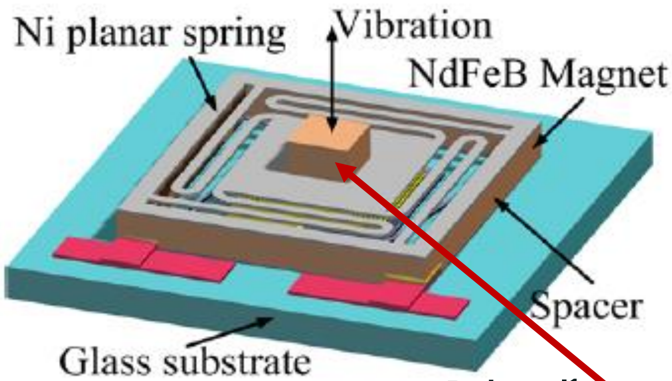

Dai et al[1]

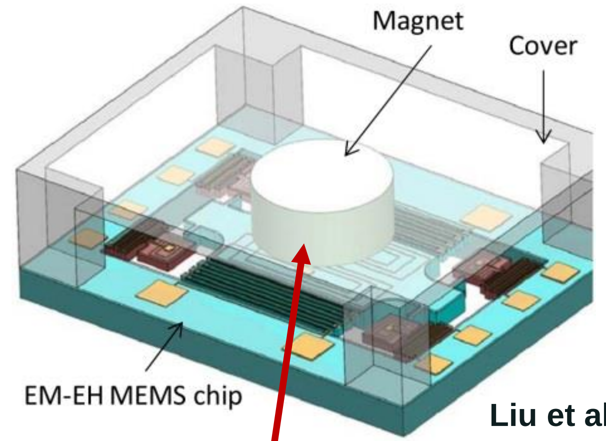

Liu et al[2]

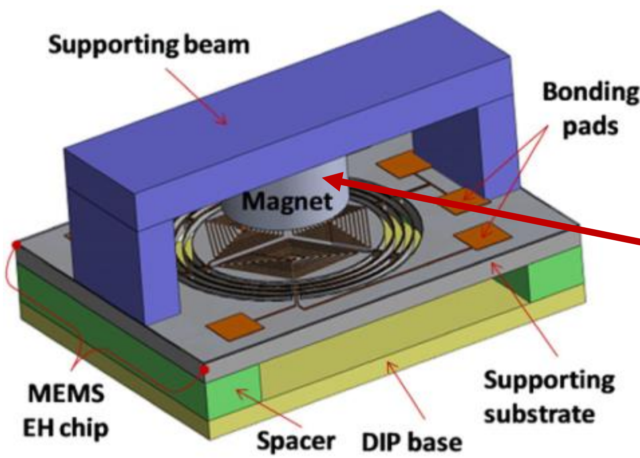

Liu et al[3]

Bulk NdFeB Magnet

- Main meso-scale element in MEMS EM-VEHs
- Barrier in batch fabrication

1. X. Dai et al., Appl. Phys. Lett., 100:031902 (2012).
2. H. Liu et al., IEEE J. Microelectromech. Syst. 23(3): 740-49 (2014).
3. H. Liu et al., J. Micromech. Microeng. 22:125020 (2012).

Material Challenges

Tyndall National Institute
Institiúid Náisiúnta

State-of-the-art Permanent Magnet Materials

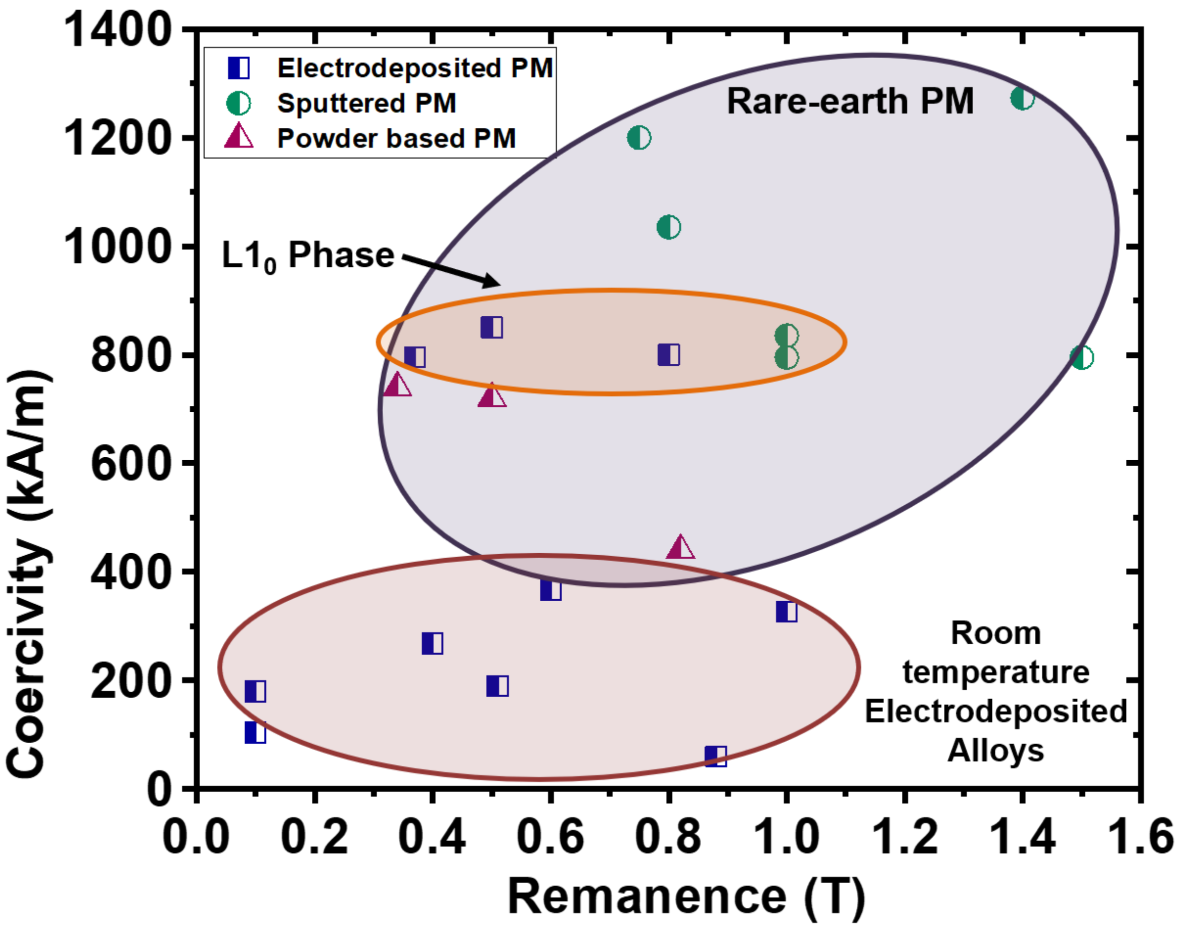

- **Rare Earth Magnets** – High Temperature processing – as such Not MEMS compatible
- **CoPt/FePt – $L1_0$ phase** – CMOS compatible deposition – High temperature (700°C) annealing
- **CoPtP/CoNiMnP/CoNiReP - Co hcp phase** – can become hard magnetic at room temperature

Integrated Permanent Magnet Development

Electrodeposition – low cost, high deposition rate

Pulse Reverse Plating (PRP) of CoPtP Permanent Magnets – Low Stress

Conventional DC Plated Film
Room Temp., 20 mA/cm²

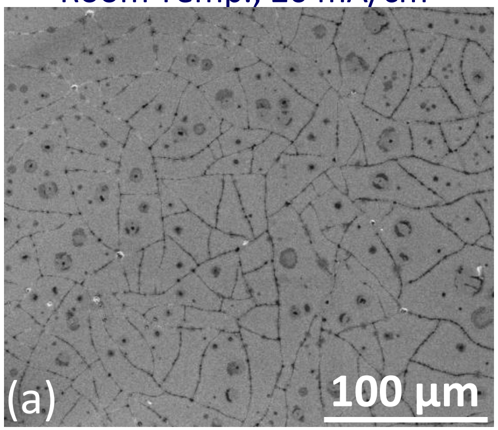

Optimized PRP Plated Film
Room Temp., 20/10 mA/cm²

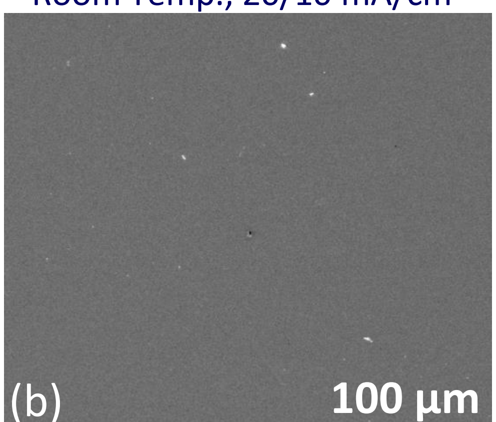

The grain size of the films increase from 6.4 nm to 22.5 nm as the thickness grows from 0.9 µm to 26 µm

Typical Reverse Pulse Waveform

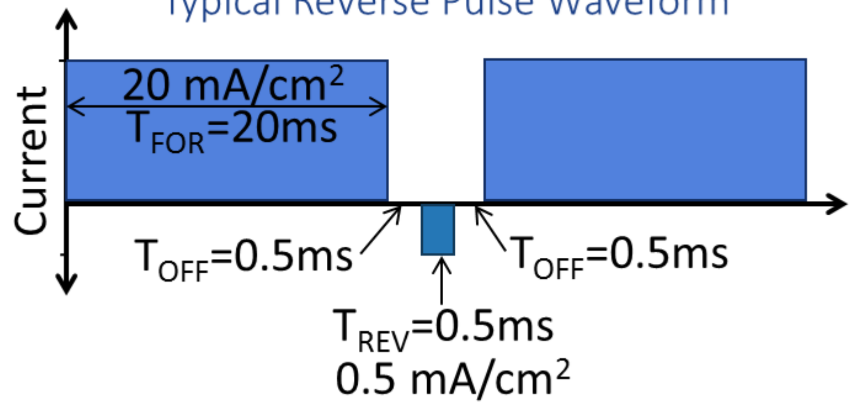

SQUID Magnetic Measurement Hysteresis Loop

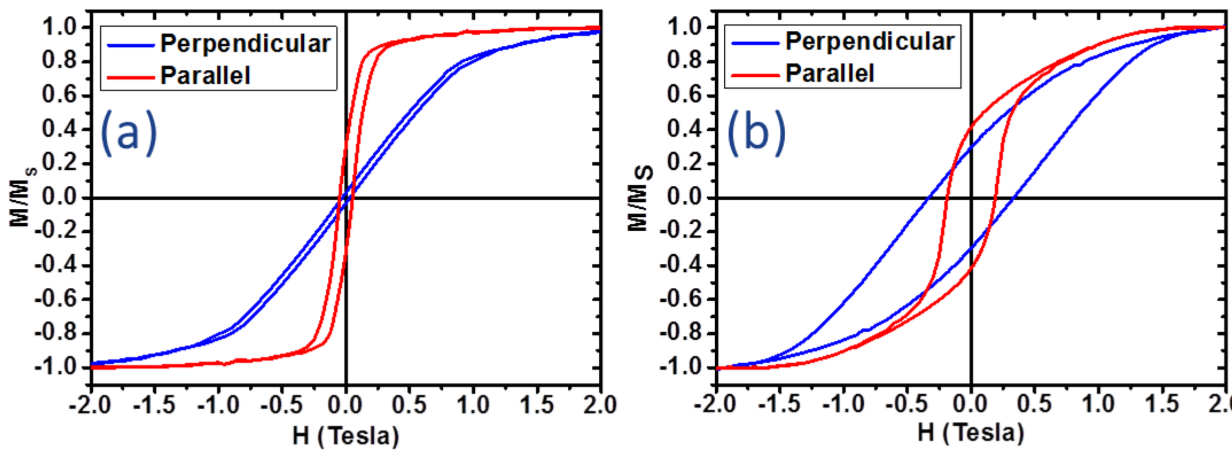

H_C (II) – 24 kA/m
H_C (⊥) – 41.4 kA/m

H_C (II) – 175 kA/m
H_C (⊥) – 268 kA/m

D. Mallick, K Paul, T Maity, S Roy, J. Appl. Phys.125, 023902, (2019)

Design Challenge – Integration of PM

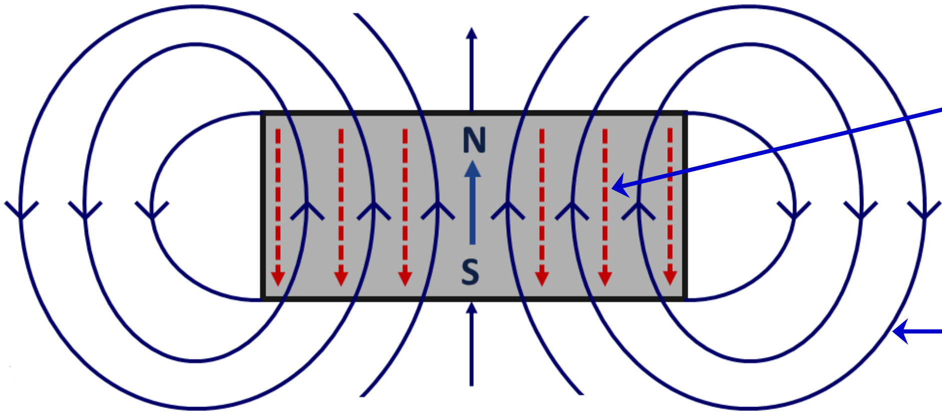

- The internal field H acting in a sample $H = H_{ext} + H_d$
  H_{ext} - External field
  H_d - Demagnetization field generated in the sample
- The demagnetization field ($H_d = -DM$) act to demagnetize the magnet in opposite to the magnetization direction
- Free magnetic poles at the terminating ends of the magnet
- Strength dependent on the magnetization and the physical magnet shape

MEMS Electromagnetic vibration energy harvester using patterned magnets

- **Solution**: Increasing the magnetic element edges while trying to retain the overall magnetization

- Replacing thin film or block of a magnetic material by Array of Patterned Magnets

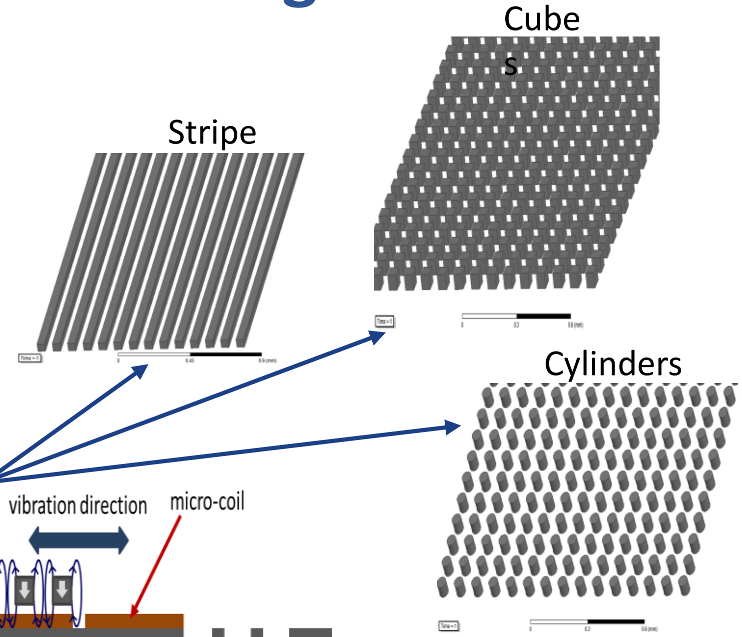

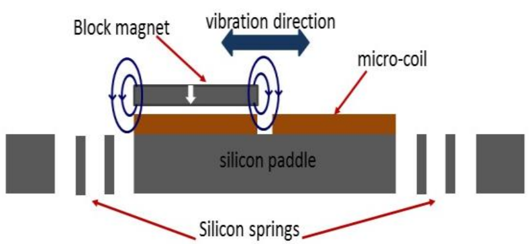

Poor performance of the integrated EM VEH due to low stray field of the block of permanent magnet

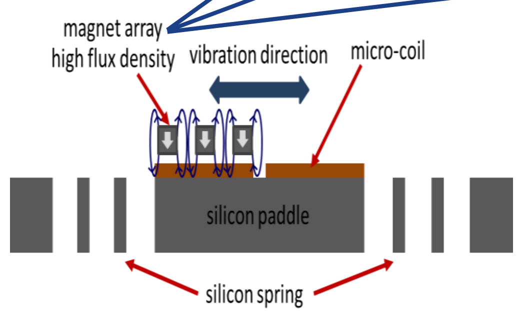

Magnetic flux density intensified over small space due to the increase of the magnetic element edges

- **Motivation**: Development and optimization of patterned magnetic micro-structures with next-generation material that shows superior hard magnetic properties.

Integration in MEMS EM VEH Structure

Finite Element Study on Magnetic Patterned Structures

Material – CoPtP; Thickness – 50 µm

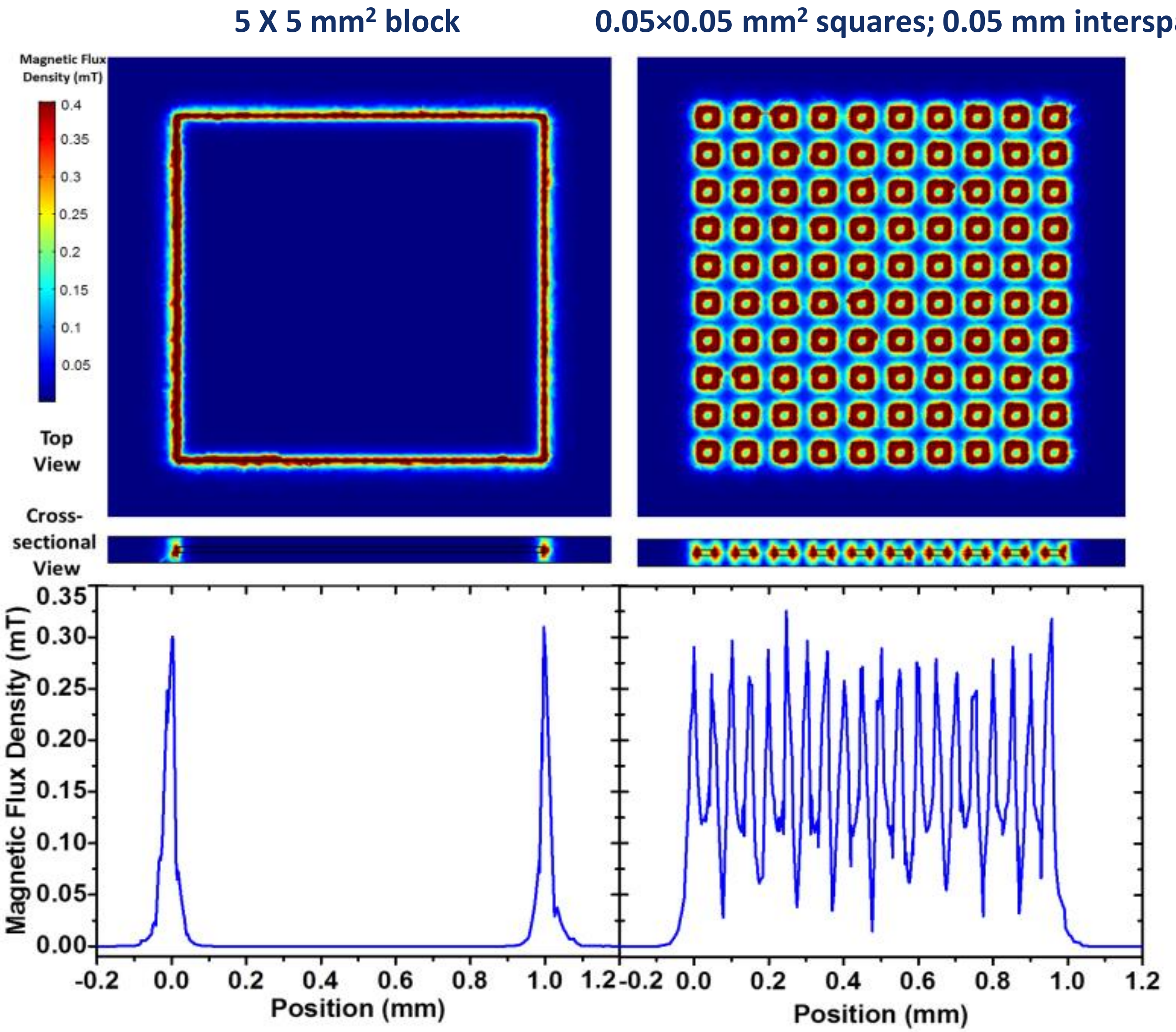

D. Mallick, K Paul, T Maity, S Roy, J. Appl. Phys.125, 023902, (2019)

Micro-patterning of MEMS scale PMs

Soft magnetic mask – pulse magnetization method

Micro-scale magnetic patterning process

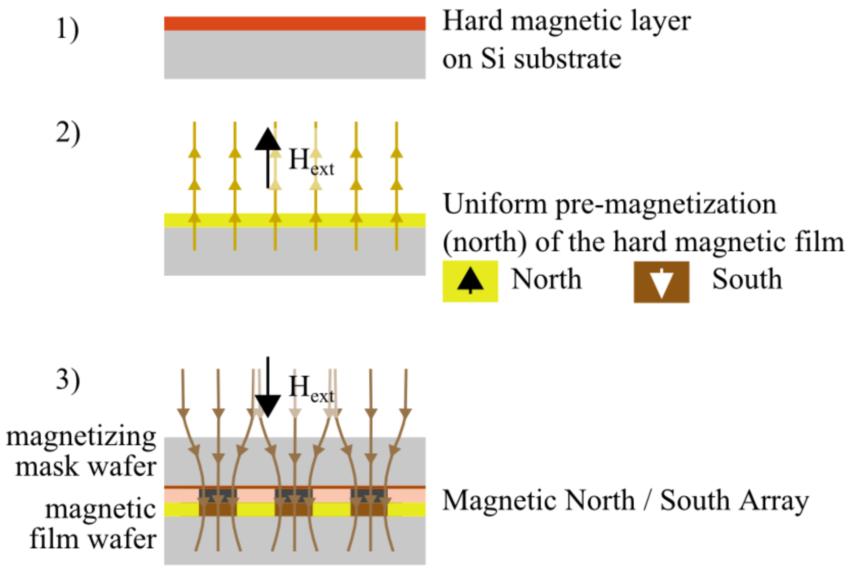

Soft-magnetic mask fabrication

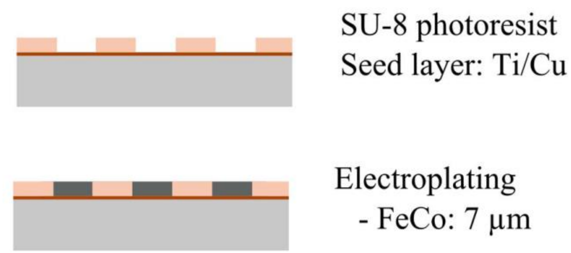

- ❖ NdFeB, CoPt PMs
- ❖ FeCo SM (Bsat = 1.3T)

Magneto optical Characterization:

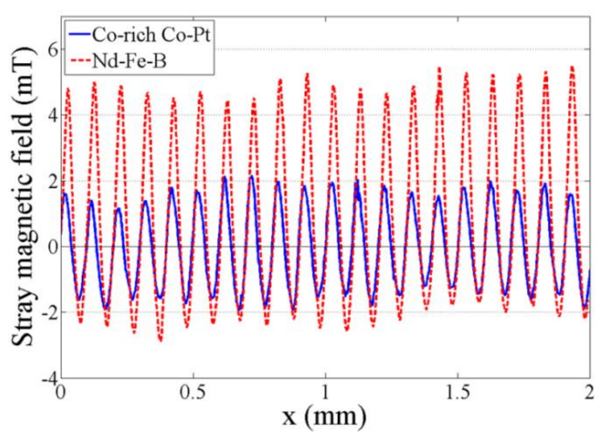

Concerns:

- Pulse reversal field – dependent on coercivity of PMs
- Diffraction during reverse pulse magnetization

O. D. Oniku et al., J. Appl. Phys., 115, 17A718 (2014)

Optimization of the magnetic structures in terms of interspacing and aspect ratio of the array

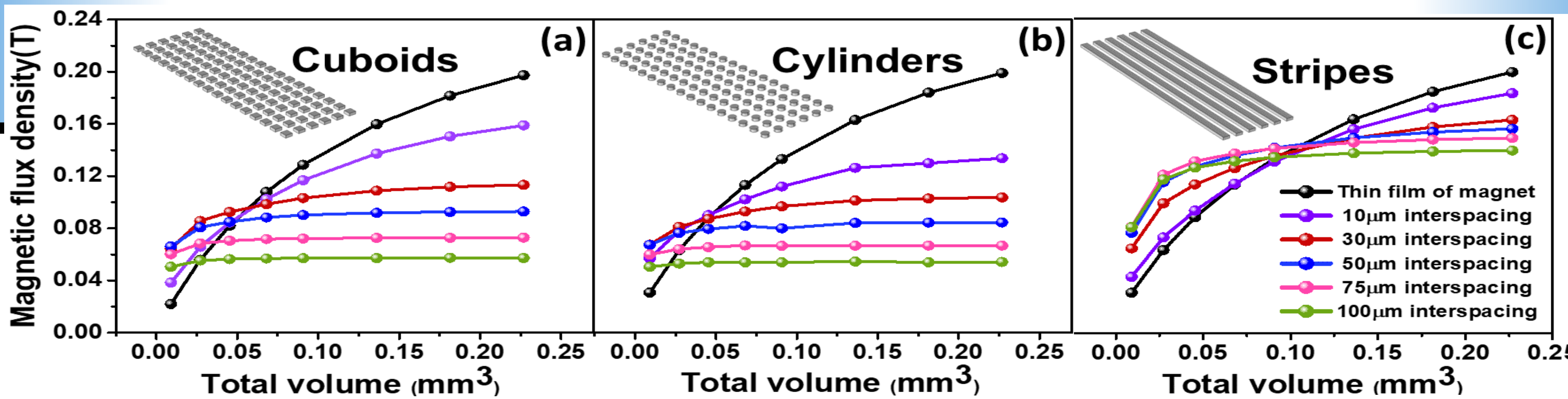

Four novel topologies for the MEMS EM-VEH

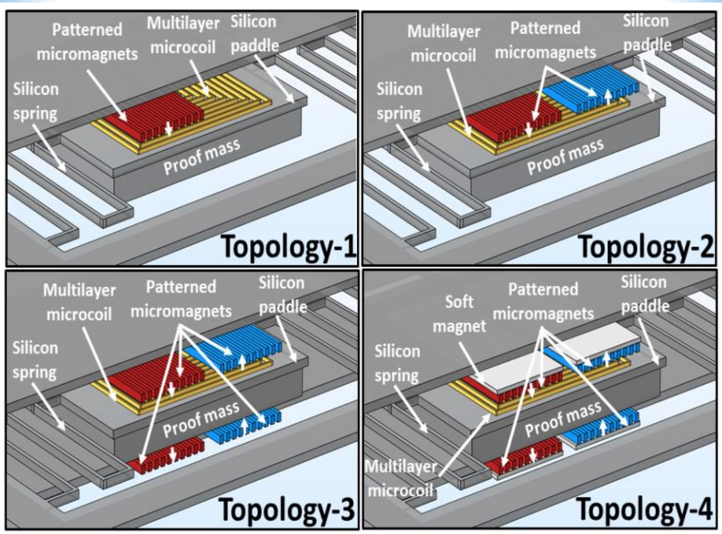

Topology	ϒ with Square coil (mWb/m)	ϒ with Rectangular coil (mWb/m)
First	2.40	10.18
Second	6.79	18.73
Third	16.21	39.40
Fourth (20μm SM)	32.60	53.03

- IEEE Power-MEMS: K Paul, D Mallick, S Roy; Dec (2019)
- IEEE Mag Lett; K Paul, D Mallick, S Roy; 12, 1-5, (2021)

Roadmap for Integrated EM VEH Devices

Invited Article: S Roy et al; *IEEE Trans. Mag.* 55, 4700315, (2019)

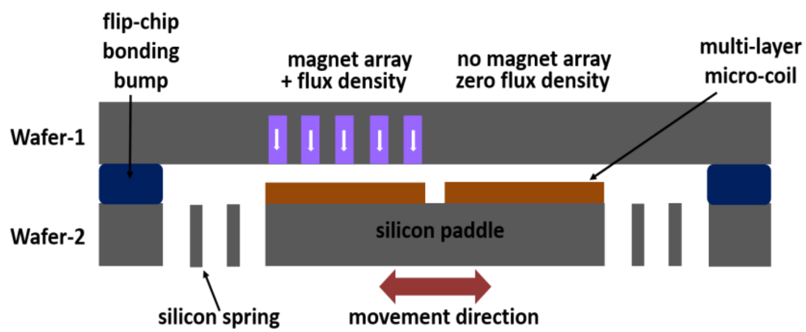

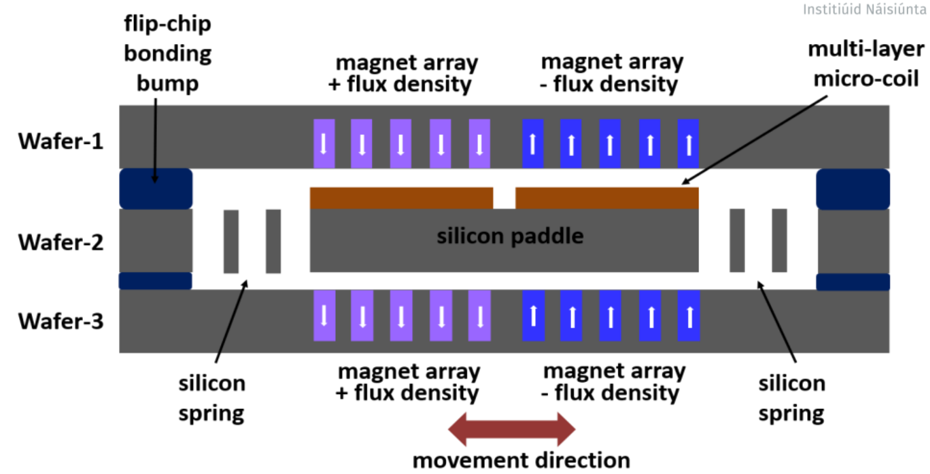

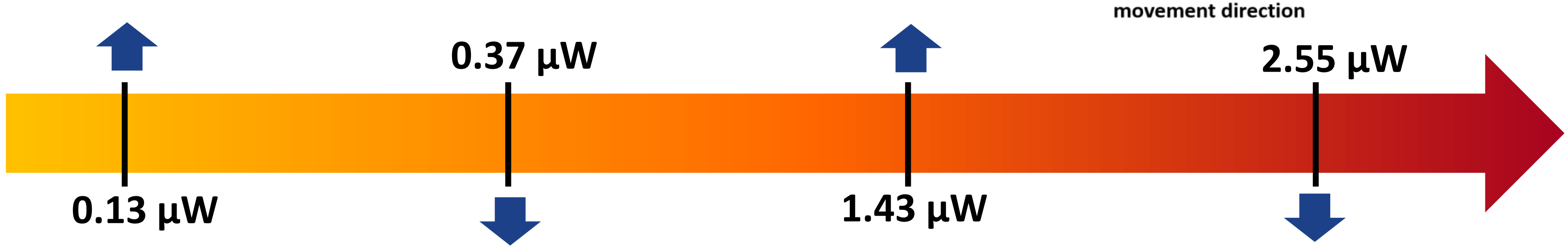

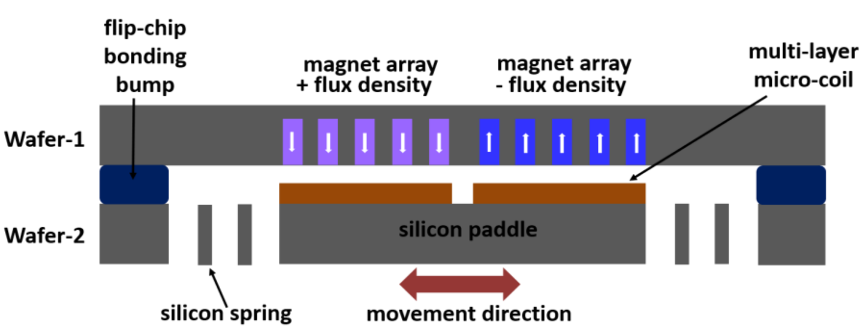

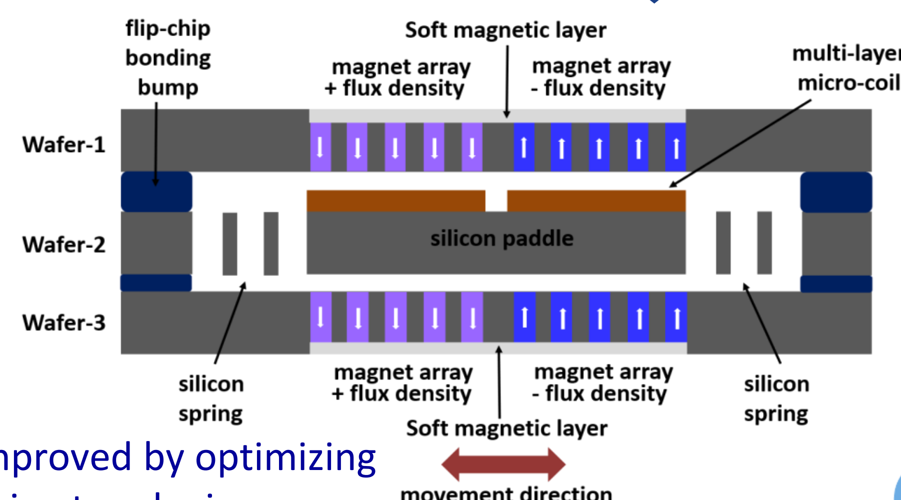

- Integrated devices can be further significantly improved by optimizing patterned magnets/coils and novel nonlinear spring topologies

Performance of linear and nonlinear MEMS EM-VEH

Comparison of different in-plane moving nonlinear spring

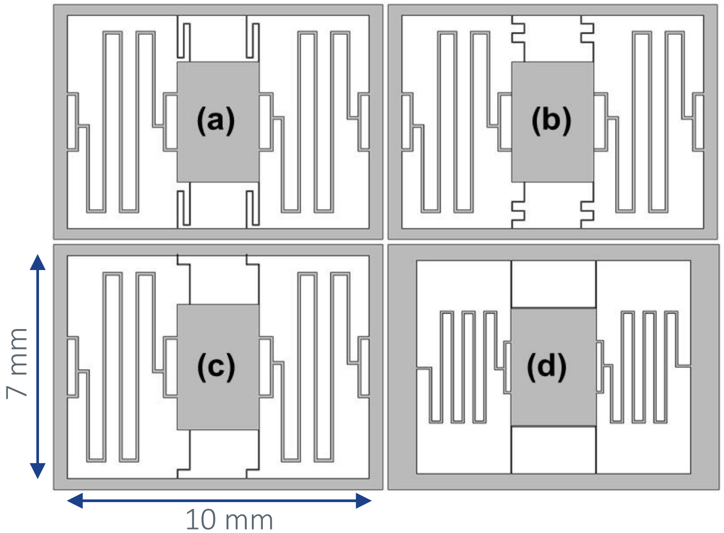

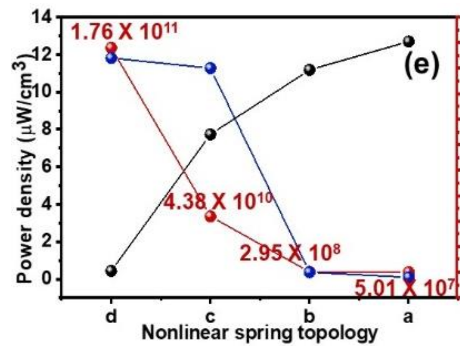

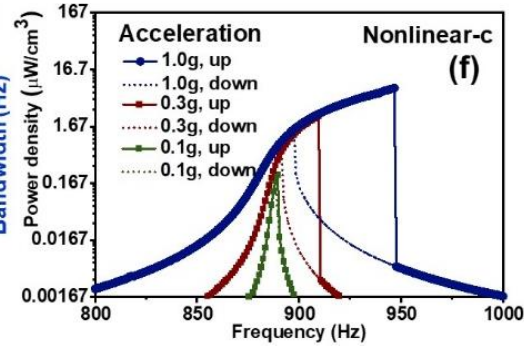

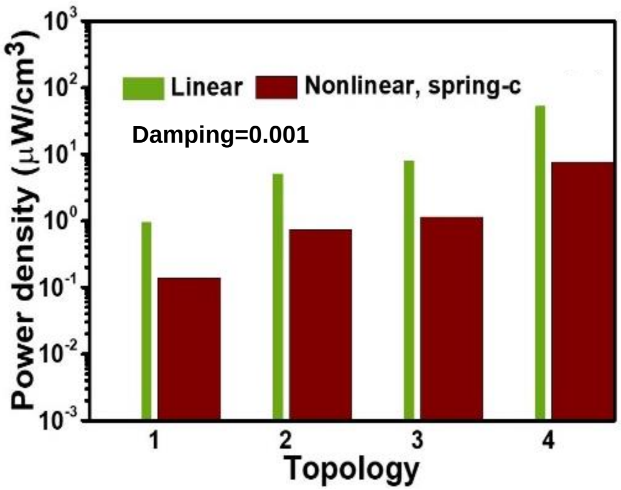

Reference	Volume (mm³)	Acceleration (g)	Resonant/ Bandwidth	Power density
[Han 2014]	67.5	1.2	Resonant peak 48Hz	0.16μW/cm³
[Liu 2013]	35	1	Resonant peak 840Hz	0.15μW/cm³
[Liu 2014]	32	3	Resonant peak 82Hz, extended up to 146.5Hz	0.056 μW/cm³
This work, linear EM-VEH	50	1	Resonant peak 614Hz, bandwidth 4Hz	52μW/cm³
This work, Nonlinear EM-VEH (spring-c)	60	1	Non-resonant, bandwidth 25Hz (921-946Hz)	7.73μW/cm³

Performance comparison of state-of-the-art MEMS EM-VEHs

❖ IEEE Mag Lett; K Paul, D Mallick, S Roy; 12, 1-5, (2021) – Funded by EU 'EnABLES' Project

Power Conversion employing micro-nano-magnetics

Evolution of Integrated Power Magnetics

Separate bobbins, windings, cores

Integration of magnetics

Planar PCB Magnetics

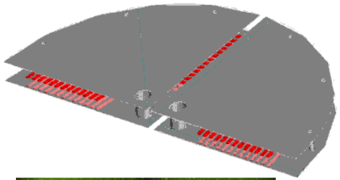

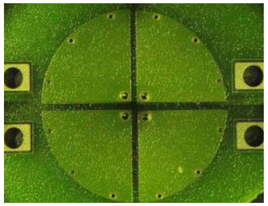

PCB Integrated Magnetics

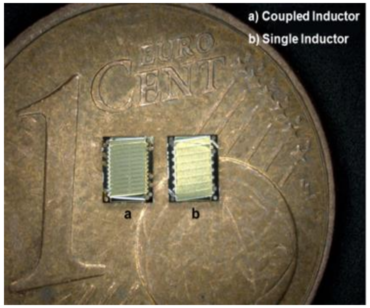

Integrated Passives on Si

Switch Mode Power Converter

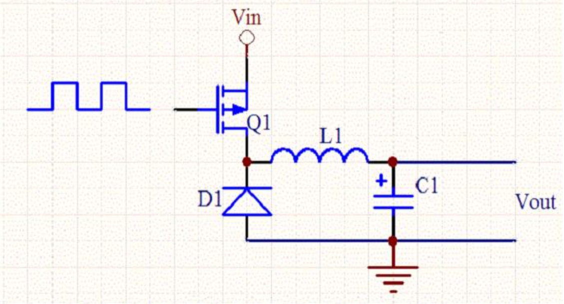

- Allowed current ripple;
- $\Delta i = (Vin - Vtrans - Vout)D/(Lf)$
- where : D = duty cycle, L= inductance, f = switching frequency.

For small *L* & high Efficiency- need high *f*

Magnetic Material - Losses

- **Hysteresis Loss**
  - **Arise from domain wall motion**
  - **Area within *B-H* loop**
  - $P_{hysteresis} = 4.\,f.B_{ac}^{2}\,H_c/B_{sat}$

Where; H_c = coercivity, B= Magnetisation, H = Magnetising field, f = frequency

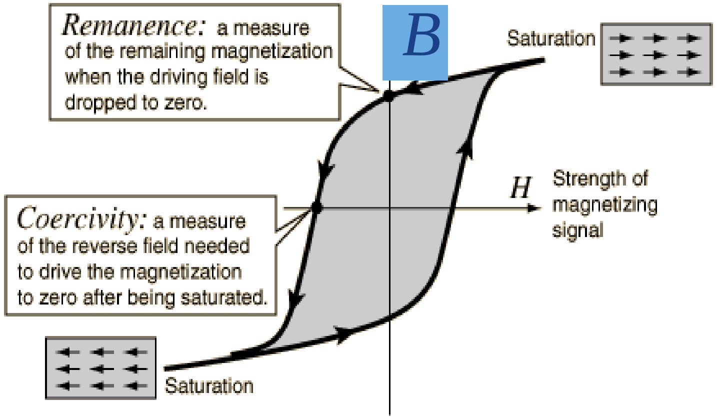

- **Eddy Current Loss**
  - **Eddy currents resist change in magnetic field**
  - **Reduced by keeping thickness below 1 or 2 skin depths**
  - **Skin depth, $\delta = (2\rho / \omega\mu_r)^{0.5}$**

Where; ρ = resistivity, ω = angular frequency ($=2\pi f$)

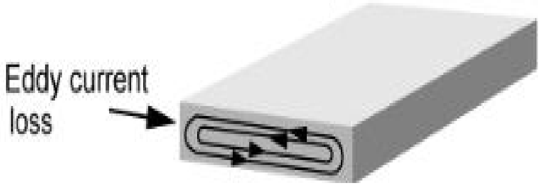

- **Anomalous Loss**
  - **Inconsistencies in domain wall motion**
  - **Often calculated as; $P_{total} = P_{hysteresis} + P_{eddy\ current} + P_{anomalous}$**

Targeted Properties for High-frequency magnetic materials

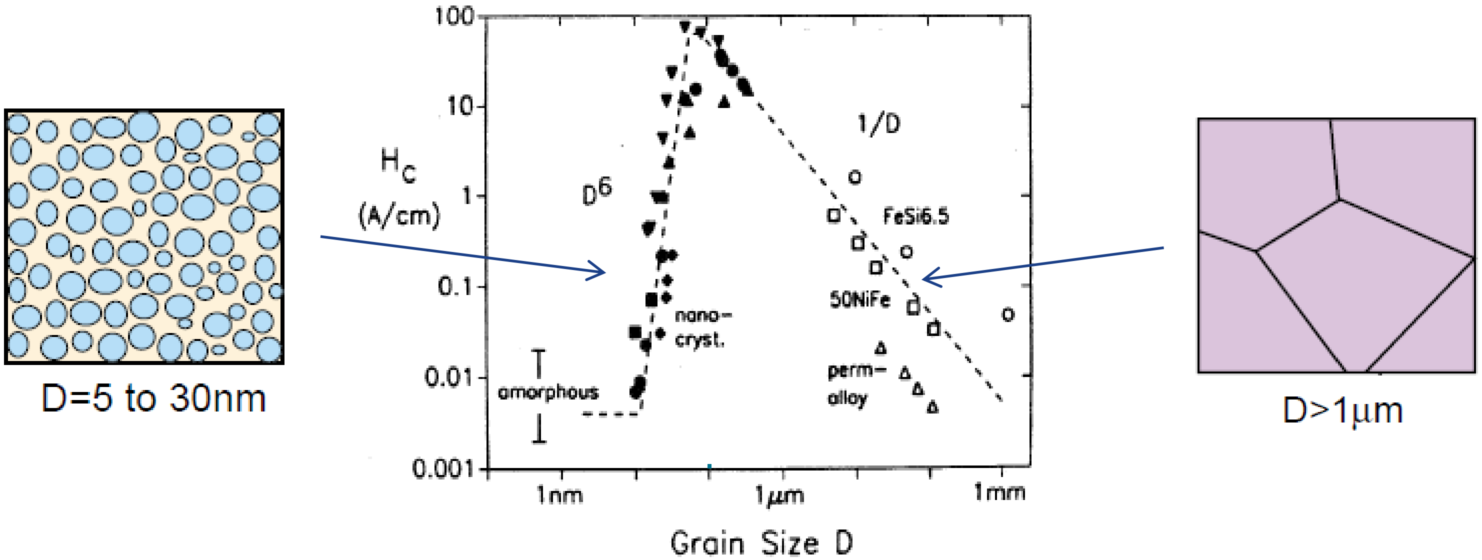

- Coercivity (Hc) < 2 Oe
- Permeability (μ_r) - 300-1000
- Saturation Flux density (Bs) – 1.5- 2.4T
- Resistivity (ρ) - 30-500 µΩcm
- Cut-off frequency for eddy current loss (*f*ed) – 100-500 MHz
- Anisotropy field (H_k) – 10-50Oe
- Natural ferromagnetic resonance frequency (f_{FMR}) – 1-3 GHz

Pulser & Pulse Reverse Plating of Magnetic Core Layers

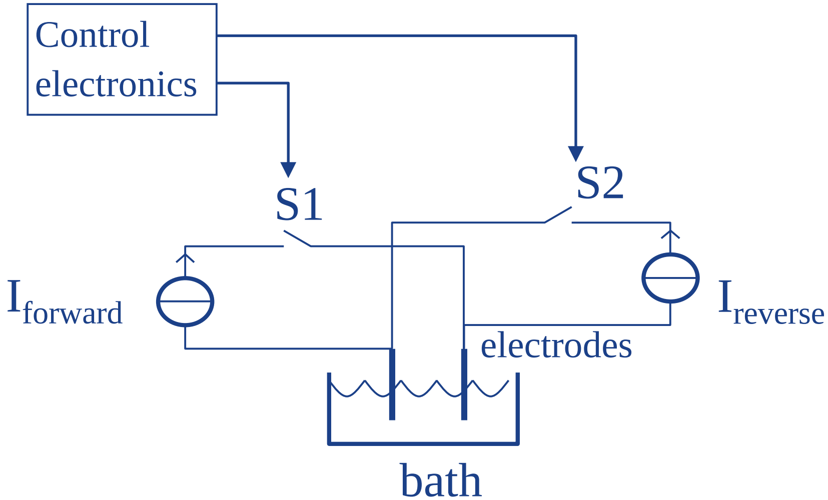


CHI 660B Potentiostat


Wafer Plating

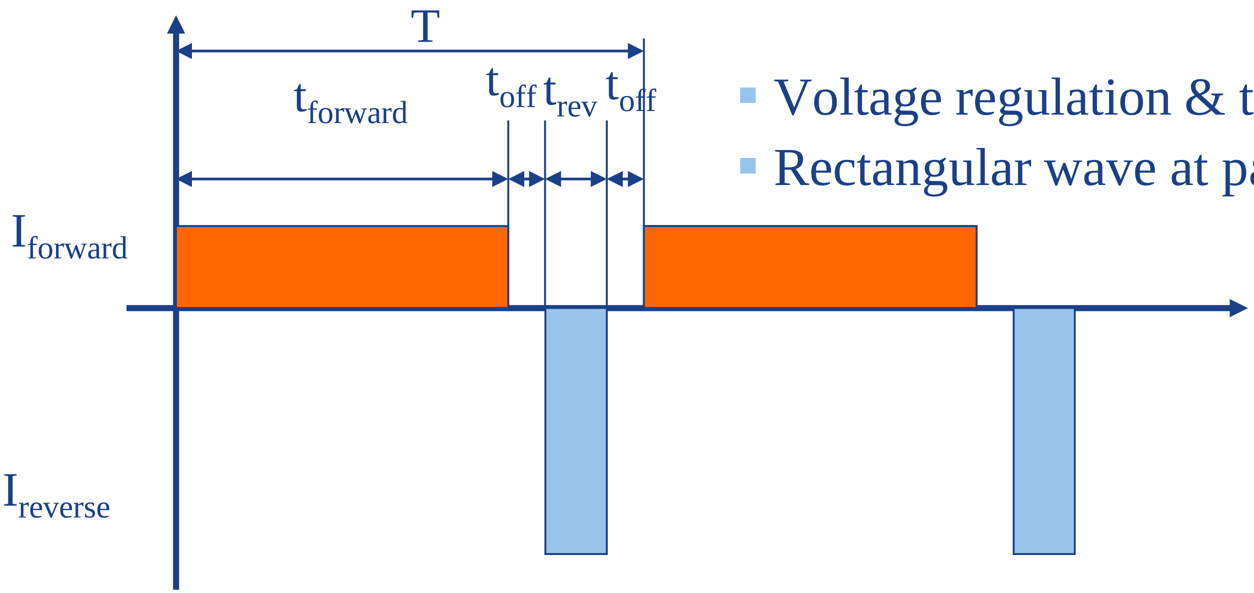

- Voltage regulation & timer circuit
- Rectangular wave at particular frequency

Nanocrystalline NiFe precessional dynamics

$Ni_{45}Fe_{55}$

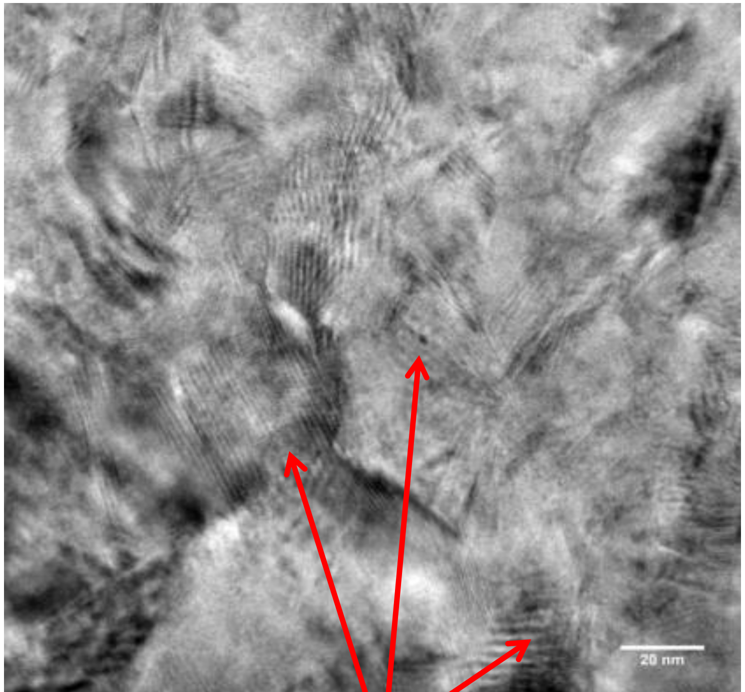

Nanocrystalline grain structure (grains ~10nm)

$$f_{FMR}^2 = \frac{\gamma^2 \mu_0^2 M_s}{4\pi^2} H_{Bias} + \frac{\gamma^2 \mu_0^2 M_s H_k}{4\pi^2}$$

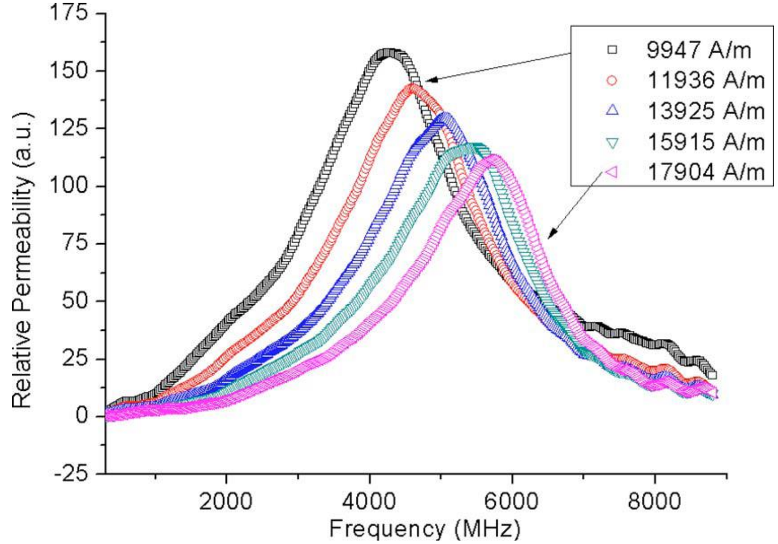

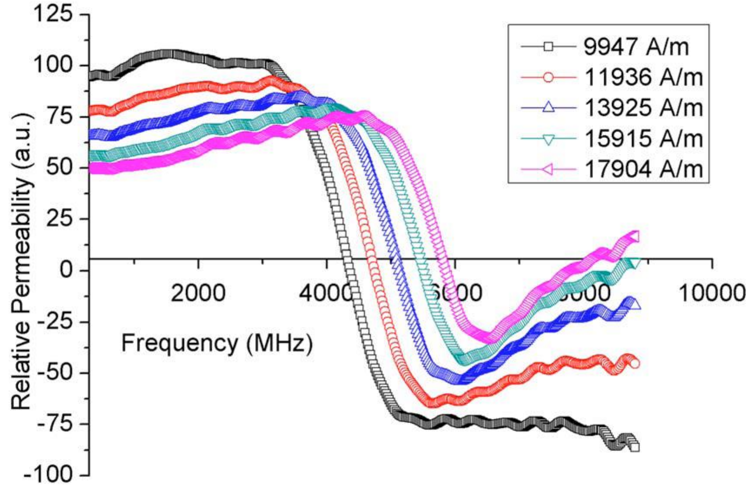

Sputtered CZTB Laminated Stack

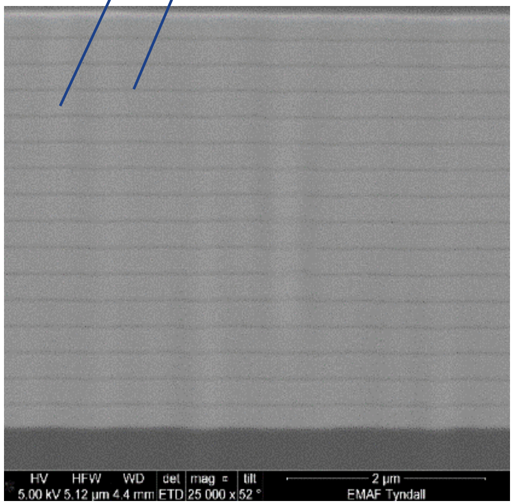

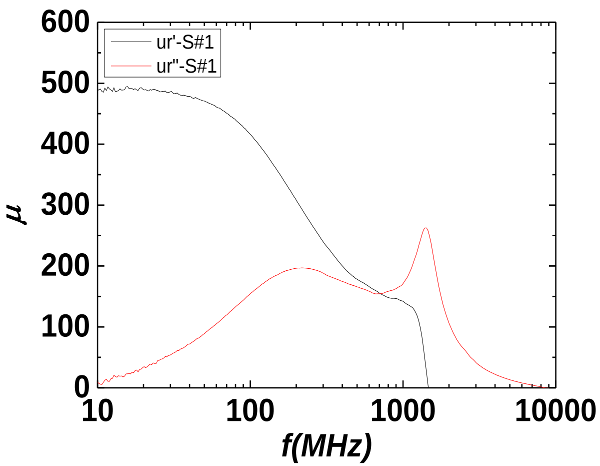

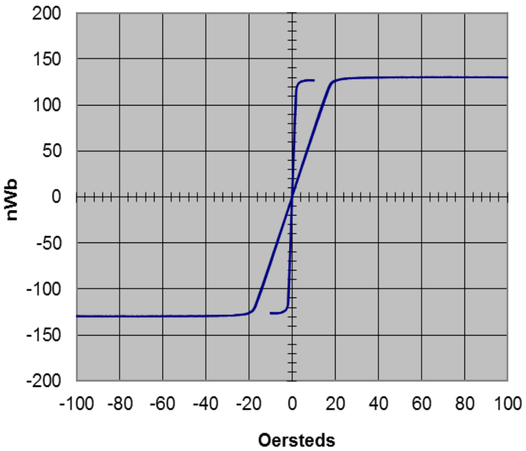

Saturation, B_s	1.2 T
Coercivity, H_c	5 A/m
Resistivity, ρ	115 µΩ cm
Permeability, μ_r	490

- Lower Hc => lower Hysteresis loss
- Higher resistivity => Lower eddy current loss
- Better frequency performance

❖ Lesker multi-target sputtering machine has been installed lately within Tyndall cleanroom with ~ €1M SFI Infrastructure grant to S Roy

Solenoid Micro-Transformer with laminated core

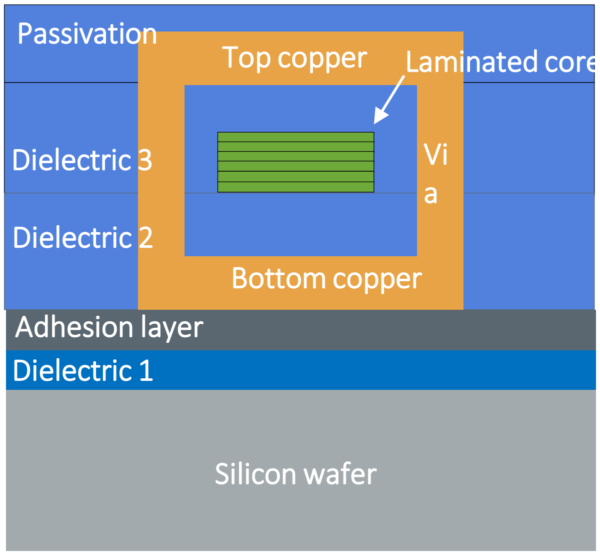

Section of solenoid structure

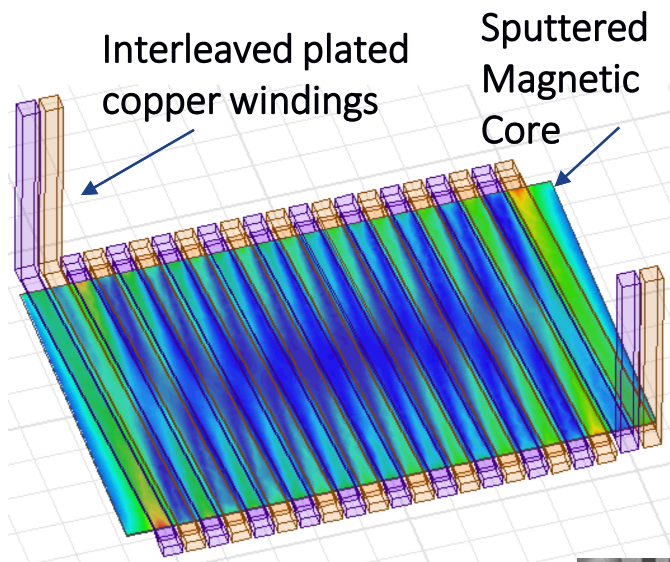

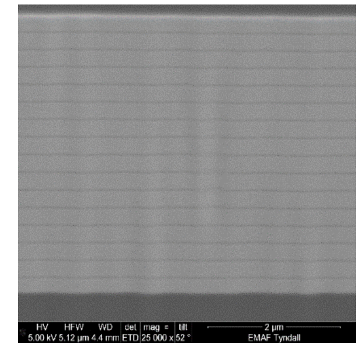

Laminated CZTB/AlN magnetic core

Advantages of a solenoid construction:-

- Laminated core fabricated on a single layer (unlike a closed core which requires two layers) => Lower cost
- No magnetic via required to connect top and bottom magnetic layers

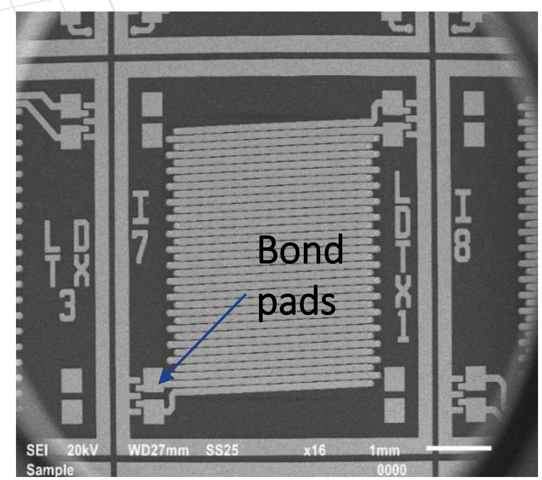

Devices prior to final passivation

Roadmap: Future Direction

MEMS EM-VEH & conversion enabled by Micro/Nano-magnetics → Powering Internet of Things (IoT)

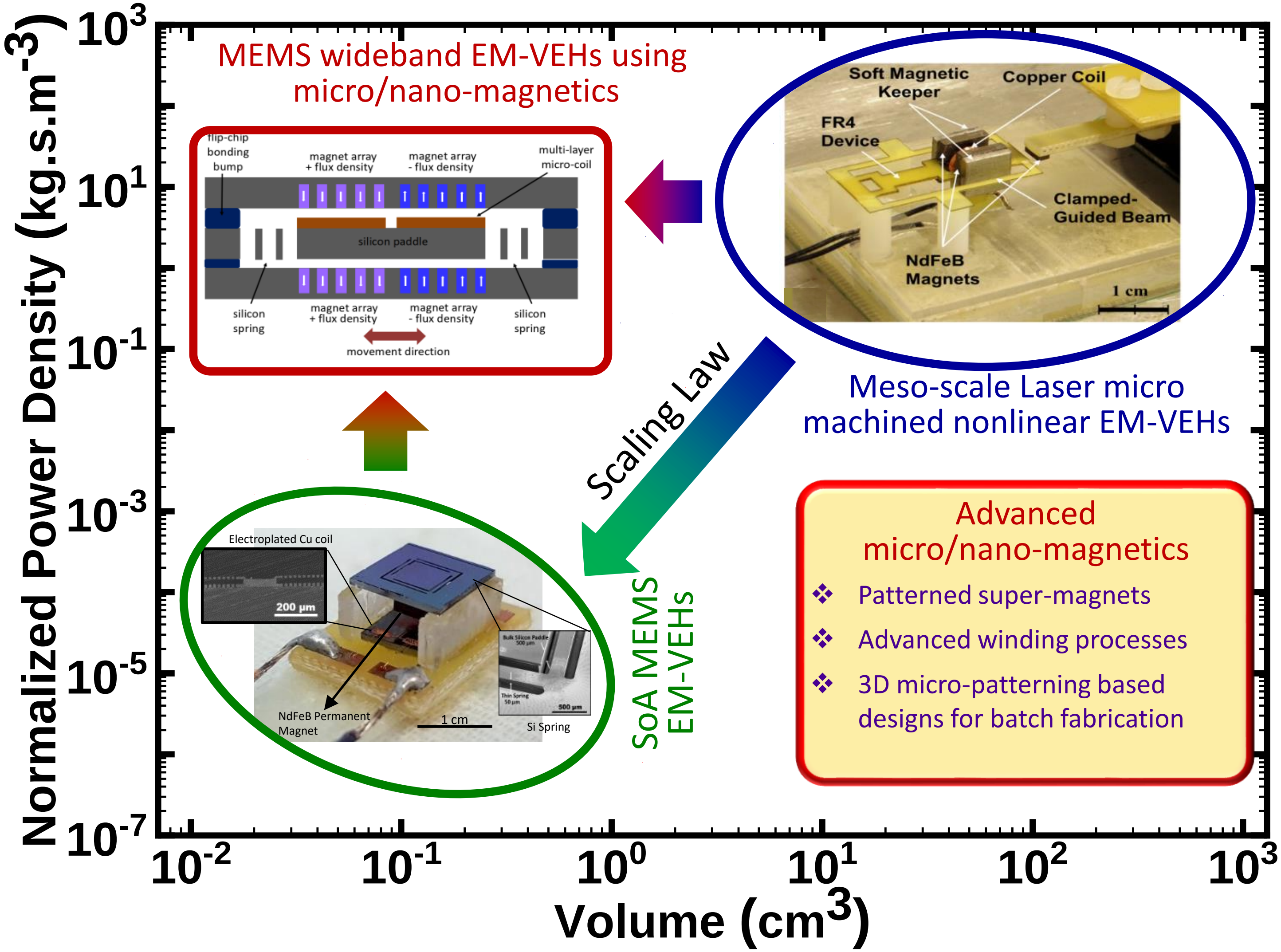

Acknowledgement:

Tyndall National Institute
Institiúid Náisiúnta

People:

Kankana Paul
Jeffrey Godsell
Pranay Podder
Brice Jamieson
Ningning Wang
Paul McCloskey
Dhiman Mallick
Santosh Kulkarni
Seamus O'Driscoll
Peter Constantinou
Tyndall Fab Facilities

Funding:

EU – H 2020 - EnABLES

EU - FP6, FP7, FET Flagship Pilot

SFI PI grant Award (2012) - 11/PI/1201

SFI TIDA grant award (2016) –16/TIDA/4174

SFI Capital Infrastructure (2013) -12/RI/2342

SFI Research Center- CONNECT- (2015 -Onwards)

Major Collaborators:

Prof. Andreas Amman - UCC, Ireland

Prof. Terence O'Donnell- UCD, Ireland

Prof. Steve Beeby – Univ. of Southampton, UK

Prof. Cian O'Mathuna – Tyndall Institute, Ireland

THANK YOU